UNCLASSIFIED

AD-A230 748

TATION PAGE

Form Approved
OMB No. 0704-0188

(Leave blank)	2. REPORT DATE	3. REPORT TYPE AND DATES COVERED
	November 1990	Final from 10/1/89 to 10/31/90

4. TITLE AND SUBTITLE
Heat Transfer Predictions of Hypersonic Transitional Flows.

5. FUNDING NUMBERS
F4962 0-90-C-0004

6. AUTHOR(S)
Joelle M. Champney

7. PERFORMING ORGANIZATION NAME(S) AND ADDRESS(ES)
Applied & Theoretical Mechanics, Inc. (ATM)
4501 Sequoyah Road
Oakland, CA 94605

8. PERFORMING ORGANIZATION REPORT NUMBER
ATM-TR-90-025

AFOSR-TR- 91 0138

9. SPONSORING/MONITCRING AGENCY NAME(S) AND ADDRESS(ES)
Air Force Office of Scientific Research
Bolling Air Force Base, D.C. 20332

10. SPONSORING/MONITORING AGENCY REPORT NUMBER
2307/A1

11. SUPPLEMENTARY NOTES

DTIC ELECTE JAN 09 1991 S B D

12a. DISTRIBUTION/AVAILABILITY STATEMENT
Distribution unlimited

DISTRIBUTION STATEMENT A
Approved for public release;
Distribution Unlimited

12b. DISTRIBUTION CODE

13. ABSTRACT *(Maximum 200 words)*

A numerical model to solve transition process observed in hypersonic flows over cones has been developed. Low Reynolds number two-equation turbulence models were employed with a production term modification (PTM) technique. The approach determined the extent of the transition zone. The onset of transition was imposed using experimental measurements when available. When not available, the onset of transition was determined by a stability criterion which is related to the Bushnell-Reshotko transition criterion. The PTM technique was incorporated into a NASA-Ames implicit Reynolds averaged Navier Stokes solver, the TURF code, and tested for transitional hypersonic flows over flat plates. The model parameters were tuned as a function of free stream Mach number. The PTM technique was also tested for transitional hypersonic flows over sharp cones and blunt cones for a variety of flow conditions. Comparisons of computed heat transfer with experimental measurements are shown to be good.

14. SUBJECT TERMS	15. NUMBER OF PAGES
transition-hypersonic-numerical-implicit-two-equation model	45
	16. PRICE CODE

17. SECURITY CLASSIFICATION OF REPORT	18. SECURITY CLASSIFICATION OF THIS PAGE	19. SECURITY CLASSIFICATION OF ABSTRACT	20. LIMITATION OF ABSTRACT
unclassified	unclassified	unclassified	unlimited

NSN 7540-01-280-5500

Standard Form 298 (Rev. 2-89)
Prescribed by ANSI Std. 239-18
298-102

UNCLASSIFIED

HEAT TRANSFER PREDICTIONS OF HYPERSONIC TRANSITIONAL FLOWS.

J.M. Champney

Applied & Theoretical Mechanics, Inc. (ATM)
4501 Sequoyah Road
Oakland, CA 94605

Research sponsored by the Air Force Office of Scientific Research (AFSR), under Contract F49620-90-C-0004. The United States Government is authorized to reproduce and distribute reprints for governmental purposes notwithstanding any copyright notation hereon.

TABLE OF CONTENTS

ILLUSTRATIONS

FOREWORD

The author wishes to thank Dr. T.J. Coakley for many useful discussions and technical advice. The author is grateful to the Applied Computational Fluid Branch at NASA-Ames Research Center for providing the computer time.

ABSTRACT

A numerical model to solve transition process observed in hypersonic flows over cones has been developed. Low Reynolds number two-equation turbulence models were employed with a production term modification (PTM) technique. The approach determined the extent of the transition zone. The onset of transition was imposed using experimental measurements when available. When not available, the onset of transition was determined by a stability criterion which is related to the Bushnell-Reshotko transition criterion. The PTM technique was incorporated into a NASA-Ames implicit Reynolds averaged Navier Stokes solver, the TURF code and tested for transitional hypersonic flows over flat plates. The model parameters were tuned as a function of free stream Mach number. The PTM technique was also tested for transitional hypersonic flows over sharp cones and blunt cones for a variety of flow conditions. Comparisons of computed heat transfer with experimental measurements are shown to be good.

1. INTRODUCTION

This research effort is to develop a numerical approach to predict heat transfer variation in the transition zone as observed on hypersonic aircraft. The accurate prediction of heat transfer on the vehicle airframe has been recognised to be critical in the development and design processes. Peak heat transfer rates and duration of heating determine the mass of thermal protection systems on spacecraft. Heating rates are strongly influenced by the boundary layer transition to turbulence, causing extremes in heat transfer and skin friction. Transition is the process by which a laminar boundary layer becomes turbulent. This process is complex because it is influenced by a variety of factors. Reference 1 gives a review of transition theory and describes various techniques employed to analyse transition.

The first theoretical idea for the analysis of transition is due to O. Reynolds and Lord Rayleigh in the 1880. Fifty years later, theoretical investigations lead to the stability theory formulated by Prandtl's school in about 1930. The next forty years saw theoretical and experimental investigations to examine transition processes. Over this period and up to the present, summaries and review papers on transition appeared but hypersonic transition received little theoretical investigations, as a result of the reduced interest for hypersonic flow regimes. Even subsonic/transonic transition received reduced attention over the last fifteen years (ref. 2). Flight test data and results of current wind tunnel experiments indicate that boundary layer transition has a major influence on the aerodynamic behaviour of hypersonic vehicles and specifically, has a major effect on:

skin friction drag,
surface heat-transfer rates,
flow separation and surface pressure distributions,
extent of shock boundary-layer interaction,
flow separation and control effectiveness,
unsteady flow phenomena,
vehicle stability and control,
surface pressure fluctuations,
structural fatigue,
acoustic noise,
and others (see Pate, ref.3).

Since the work of Kovasnay in 1953 (ref. 4), the response of the boundary layer to environmental disturbances is now believed to be the dominant criterion of the transition process (see work by Stetson, ref. 5). In flight, disturbances have much lower freestream disturbance levels than conventional supersonic-hypersonic wind tunnels. Experimentalists in hypersonic transition have devoted much effort to reduce facility free-stream disturbances to low levels, approaching those in flight (ref. 6). The paper by Dougherty and Fisher (ref. 7) reviews wind tunnel flight data correlations and is a useful source of data.

Free-stream disturbance effects need to be incorporated into a transition model. The present work is an attempt to model the interaction of the free-stream disturbances and turbulence with boundary layers on flat plates and cones, making use of experimental data and recent advances in Computational Fluid Dynamics.

Kovasnay identifies three primary disturbance sources in wind tunnels: vorticity fluctuations (free-stream turbulence), entropy fluctuations and sound waves. The paper by Pate (ref. 3) presents a review of these effects. Figure 1 extracted from Pate paper, summarizes the dominant effects of flow disturbances as a function of Mach numbers and as observed in wind tunnels. It can be seen in Figure 1 that the radiated noise is the dominant free-stream effect of the boundary layer transition processes for the Mach numbers of interest in this effort, i.e. greater than 3. The importance of temperature fluctuations is not well understood at the present time.

In this research effort, the transition model developed by Schmidt and Patankar (ref.8) for incompressible flows, was tested and modified for transitional hypersonic flows using experimental data with the most influencial factor in the model taken to be the level of noise converted into free-stream turbulence intensity. The approach employs a production term modification (PTM) which consists of a modification to low Reynolds number (LRN) two-equation models. A modification to the production term in the modeled turbulence field equations is correlated to the free-stream turbulence level using experimental data. The modification does not affect the fully turbulent calculations and greatly improves the transition predictions. The approach is discussed in the following section.

2. TECHNICAL APPROACH

2.1 The numerical model.

The computer code selected for this effort is the NASA-Ames TURF code developed by T.J. Coakley (refs. 9 and 10). The TURF code is an implicit finite difference code for solving the Reynolds averaged compressible Navier-Stokes equations and incorporates several zero- and two-equation turbulence models. The code solves the two-dimensional (2D) and axisymmetric equations using a finite volume approach and an approximately factored alternating direction implicit (ADI) algorithm. Second-order upwind differencing is used for inviscid flux differencing (closely related to the flux difference splitting approach of Roe) and central differencing is used for the viscous terms. The implicit operator utilises a non-conservative diagonal form, first order upwind differencing of inviscid terms and an approximate (diagonalised) second-order differencing of viscous terms.

ATM examines the possibility of replacing the left hand side (LHS) operator of the TURF code by a lower-upper symmetric successive overrelaxation (LU-SSOR) technique, as developed by Yoon and Jameson (ref. 11). In this technique, the Navier-Stokes equations are differenced and not factored as in the ADI methods. The technique was, at first, attractive because it is a two factor (or sweep) scheme even in three dimensions (3D), and it is theoretically unconditionally stable in 3D. This was found not to be verified for simple two dimensional flows, it was not possible to use a large time step. Various forms of the implicit operator were tested using at first u, u+c, u-c, v, v+c, v-c, for the inviscid eigenvalues of the matrices that appear in the differencing of the LHS operator, u is the streamwise (or x) velocity component, v is the normal (or y) velocity component, c is the sound speed. The computation was unstable and could use only a small time step corresponding to a Courant-Friedrichs-Levy number of 1. If each eigenvalue is replaced by its largest value, then the time step can become infinite, however, the rate of convergence to a steady state solution is slow, slower than the original TURF upwind ADI algorithm. T.J. Coakley and George Hwang at NASA-Ames Research Center have pursued extensive investigations of the LU-SSOR algorithm that lead to the implementation in the TURF code of a Gauss Seidel line relaxation technique for the LHS operator. In their applications, the new algorithm allows an infinite time step, but even with the infinite time-step, the code still converges in roughly the same number of time steps than the original TURF code. In addition, the Gauss Seidel technique is not vectorizable in 2D on the NAS CRAY, and uses more computer time than the TURF algorithm. For theses reasons and following T.J. Coakley recommendations, it was decided to keep in the TURF code, the original LHS implicit ADI operator.

2.2 The PTM technique.

The purpose of this section is to describe the mathematical implementation of the PTM technique in the low Reynolds number Jones-Launder k-ϵ turbulence model, k is the turbulent kinetic energy and ϵ is the dissipation rate of k.

The basic relation defining the turbulent viscosity μ_T, is

$$\mu_T = \rho \, C_\mu \, f_\mu \, \frac{k^2}{\epsilon}$$

ρ is the density, C_μ is a constant equal to 0.09, f_μ is a low Reynolds number function or damping function.

$$f_\mu = \exp\left(\frac{-3.4}{(1+0.2R_T)^2}\right)$$

R_T is the turbulent Reynolds number and is equal to $k^2/\nu\epsilon$, ν is the kinematic viscosity equal to μ/ρ, μ is the molecular viscosity given by Sutherland law.

The unsteady transport equations for k and ϵ are, in 2D:

$$\frac{\partial \rho k}{\partial t} + \frac{\partial}{\partial x}\left\{\rho k u - (\mu + \frac{\mu_T}{\sigma_k})\frac{\partial k}{\partial x}\right\} + \frac{\partial}{\partial y}\left\{\rho k v - (\mu + \frac{\mu_T}{\sigma_k})\frac{\partial k}{\partial y}\right\} = P_k - \rho(\epsilon + D)$$

$$\frac{\partial \rho \epsilon}{\partial t} + \frac{\partial}{\partial x}\left\{\rho \epsilon u - (\mu + \frac{\mu_T}{\sigma_\epsilon})\frac{\partial \epsilon}{\partial y}\right\} + \frac{\partial}{\partial y}\left\{\rho \epsilon v - (\mu + \frac{\mu_T}{\sigma_\epsilon})\frac{\partial \epsilon}{\partial y}\right\} = \frac{\epsilon}{k}\left\{C_1 f_1 P_k - \rho C_2 f_2 \epsilon\right\} + E$$

P_k is the production of k and is equal to: $\mu_T S^2 - (2/3)\rho k D$.

$$D = u_{k,k} = \frac{\partial u}{\partial x} + \frac{\partial v}{\partial y} \qquad S^2 = (u_{i,j} + u_{i,j})u_{i,j} - \frac{2}{3}D^2$$

$$f_1 = 1.\ ,\ f_2 = 1.-0.3\exp(-R_T^2)\ ,\ D = \frac{2\nu}{\epsilon}\left(\frac{\sqrt{k}}{\partial y}\right)^2\ ,\ E = 2\mu_T \nu \left(\frac{\partial u}{\partial y}\right)^2$$

$C_1 = 1.44$, $C_2 = 1.92$, $\sigma_k = 1.0$, $\sigma_\epsilon = 1.3$.

t is the time, the indices i, j, k indicate the i, j, k directions and can be equal to 1 (i.e., x) or 2 (i.e., y).

ATM experimented with the Chien, Lam-Bremhorst and Jones-Launder models (refs. 12-14) for flat plate flows and did not find any difference between the models that could allow to define one of the models as the "best" model for this study. Consequently, in the applications reported here, the Jones-Launder model was used because it is the oldest two-equation model and has been widely used.

A basic difference between the three models is that they each use different LRN functions for f_μ, f_1, f_2, E, D. Another difference between the three models is that in the Chien and Jones-Launder models, the variable ϵ is a modified dissipation

function, so that its value at the wall can be set to zero. In the Lam-Bremhorst model, ϵ retains its original definition which leads to zero-gradient boundary condition on ϵ at the wall.

Initial and far field conditions. The stability of a two-equation model computations is usually related to the free stream values of the turbulent variables: k_∞, ϵ_∞ and μ_{T_∞}, ∞ denotes free stream values. The following values are used for initial conditions:

$$k_\infty = \frac{1}{2}\,(TUE*U_\infty)^2 \quad , \quad \mu_{T\infty} = 0.01\ \mu \quad , \quad \epsilon_\infty = RSR*\mu_T/(C_\mu \rho k^2)$$

TUE is the free stream turbulence level that can vary from 0.1% to 6%. The stability of the computation is usually related to the value of ϵ_∞. With the Jones-Launder model, if ϵ_∞ is too large, turbulence is destroyed and the flow remains laminar, if ϵ_∞ is too small, the computation becomes unstable. There is therefore, an optimum value of ϵ_∞. In our computations, it was found that an appropriate value of ϵ_∞ corresponds to the constant RSR equal to 0.001 or 0.01. The k-ϵ solution does not depend upon these values. In the far field, k and ϵ are set to their initial values. In the flow field, they are prevented from becoming smaller than k_∞ and ϵ_∞.

Generally, two-equation models, when applied to transitional flows over flat plates, predict laminar flow followed by fully turbulent flow. In the present applications, ATM found that the two-equation models predict fully turbulent flow starting at the leading edge of flat plate flows, when crude initial conditions are used, i.e. the flow variables are set to constant values. If initial conditions are refined using known analytical solutions for the flow variables, the two-equation models will predict laminar flow followed by fully turbulent flow. In all cases, the transition zone is very narrow. This is translated by a sharp increase of skin friction and heat transfer. The profiles of turbulent kinetic energy, k, along flat plates, in the laminar region show a very slow increase from zero at the wall up to the boundary layer edge value. Downstream, the k-profiles undergo the rapid development of a peak inside the boundary layer: turbulent kinetic energy from the free stream is convected and diffused into the boundary layer. In this process the production of k in the two-equation model becomes significant and larger than the dissipation of k. The process is self generating causing a rapid increase of k. It is necessary therefore to modify the production term of k in the k and ϵ equations to improve predictions of transition processes.

The PTM technique is employed in conjunction with a two-equation model. The PTM technique limits the growth rate of P_k, using a linear relationship depending on P_k:

$$\left[\frac{\partial P_k}{\partial t}\right] \cong \frac{\Delta P_k}{\Delta t} = A\ P_k + B \qquad (1)$$

A and B have the dimension of the inverse of time.

Another way to compute the growth rate of P_k is to use the following equation:

$$\frac{\Delta P_k}{\Delta t} = \frac{P_k^{n+1} - P_k^n}{\Delta t} \qquad (2)$$

where Δt is the computational time step (=dx/u where dx is the stepsize in the streamwise direction).

P_k^n is the production of k at time n resulting from the use of the PTM technique.

P_k^{n+1} is obtained from the product of the Reynolds stresses with the gradients of the mean velocity.

The PTM technique determines the value of P_k at x+dx to be used over the next step in the solution, by adding to the value of P_k at x, the smallest increment (ΔP_k) for the growth rate of P_k, obtained from equation 1 or 2.

Equation 1 is employed in the transition zone, characterised as the zone where the calculated Reynolds number based on momentum thickness, $R_{e\theta}$, is greater than a critical Reynolds number, $R_{e\theta,c}$ (equal to 162 for incompressible flows).

If $R_{e\theta}$ is less than $R_{e\theta,c}$, the growth rate of P_k is set to zero and the two-equation model will predict laminar flow. When the growth rate of P_k calculated by (1) becomes larger than the growth rate of P_k given by Equation 2, Equation 1 is not used anymore, leaving the two-equation model unmodified by the transition model, in fully turbulent flow.

In Equation 1, the two parameters, A and B, are made dependent upon the free-stream turbulence intensity and were determined using the correlation of Abu-Ghannam and Shaw (ref. 15), which is a criterion for $R_{e\theta}$ to determine the start and the end of transition.

The A and B parameters were derived in reference 8 and are given below.

Let $\phi = 100 * Tu_E$, $\bar{B} = \bar{B} * 10^{12}$, and $\bar{\mathcal{A}} = \bar{A} * 10^{6}$

$0.0 < \phi < 2.0$	$\log_e(\bar{B}) = -5.8084 + 2.995*\phi$
$2.0 < \phi < 6.0$	$\bar{B} = 18.738 - 26.8085*\phi + 12.7536*\phi^2 - 2.1152*\phi^3 + 0.1218*\phi^4$
$6.0 < \phi$	$\log_e(\bar{B}) = 1.950 + 0.1573*\phi$

$0.0 < \phi < 6.0$	$\bar{\mathcal{A}} = 12.2266 - 1.7904*\phi - 2.4229*\phi^2 + 0.57595*\phi^3 - 0.0365*\phi^4$
$6.0 < \phi$	$\bar{\mathcal{A}} = -7.5 - 0.19*\phi$

$\bar{A}$ and $\bar{B}$ are the non dimensionalized A and B parameters with respect to local free stream conditions involving the density, the velocity and the molecular viscosity:

$$\bar{A} = \frac{A\mu_e}{\rho_e U_e^2} \quad , \qquad \bar{B} = \frac{B\ \mu_e^2}{\rho_e^3\ U_e^6}$$

Figures 2 and 3 give the variation of A and B as a function of TUE for the Jones-Launder model.

From Equations 1 and 2, it can be noted that the time dependency is built in the model to slow down the transition process. The time scale is related to the local velocity. The PTM technique verify some experimental evidences (ref. 8):

- Free stream turbulence influences the transitional flow.
- When the free-stream turbulence intensity increases, the transition region moves upstream, skin friction and Stanton number increase too.
- In accelerating free stream flows (favorable pressure gradient) the transition moves downstream, the transition zone is longer because of the stabilizing effects of accelerated freestream flows.
- The process of transition, once started, evolves at a finite rate, the rate at which P_k changes is limited.

Schmidt and Patankar compared their incompressible model against experimental measurements for 34 low speed flow experiments. In most cases, the agreement of skin friction and heat transfer is good, if not excellent. In the present approach, compressibility effects are treated in terms of Favre (mass-averaged) variables and the gas is assumed perfect with a constant "gamma", therefore, Favre averaging is appropriate. The use of Favre averaging is a controversial issue in the turbulence modeling of hypersonic flows because hypersonic flows involve multiple reacting species interacting with turbulence. Favre averaging tends to oversimplify the partial differential equations, important terms might disappear. However, this very complex issue is not addressed in this work.

2.3 Conversion of noise level into free stream turbulence.

To apply two-equation turbulence models, a value of the free-stream turbulence level, is needed in the far field to start the computation of the turbulent kinetic energy k and to set the far field boundary conditions. In addition, the PTM model includes two constants that depend upon the free stream turbulence level. In hypersonic flow, the noise level is assumed to be the dominant influencial factor and is related to the free stream fluctuating pressure. The free stream turbulence is related to the free stream velocity fluctuation. The noise level is now measured by experimentalists in wind tunnels and it is therefore desirable to relate the noise level to a free stream turbulence level to perform numerical simulations with two equation models. Laufer (ref. 16) derives a relation assuming that the free stream disturbance is a plane wave propagating at a Mach number relative to the free stream. Using the unsteady Bernoulli equation, an equation between fluctuating velocity and fluctuating pressure is obtained. This relation, used by Shamroth and MacDonald (ref. 17), involves a factor treated as an integral of a space-time correlation function which is difficult to evaluate and crude assumptions have to be made. Therefore, a simple analysis to relate the fluctuating pressure and TUE was performed using a one dimensional perturbation technique of the steady Bernoulli equation. A perfect gas is assumed, temperature fluctuations are neglected. The steady inviscid Bernoulli equation is assumed verified in wind tunnels in the free stream and is written as:

$$\frac{p}{\rho} + \frac{1}{2}\rho q^2 = \text{constant}$$

The variables pressure, p, density, ρ, and magnitude of the velocity, q, are perturbed from their free stream values:

$$p = p_\infty + p' \ , \ \rho = \rho_\infty + \rho' \ , \ q^2 = (U_\infty + u')^2 + v'^2 + w'^2$$

with $u' >> v'$ and $u' >> w'$. The perturbed Bernoulli equation

becomes:

$$\rho_\infty U_\infty u' + 0.5\, \rho' U_\infty^2 = 0$$

that leads to : $$TUE = \frac{\overline{(u'^2)}^{1/2}}{U_\infty} = \frac{1}{2} \frac{\overline{(p'^2)}^{1/2}}{p_\infty}$$

With this crude analysis, the experimental data of rms pressure fluctuations versus Mach number as given in Figure 4 can be used to obtain the fluctuating pressure for a given Mach number and subsequently the value TUE needed in the numerical simulations.

2.4 The stability criterion

The PTM technique employs a stability criterion stating that for a Reynolds number based on momentum thickness, $R_{e\theta}$, less than a critical value, $R_{e\theta,c}$, the production term of k is set to zero.

For incompressible flows, $R_{e\theta,c}$ was selected to be 125 (ref. 8). For hypersonic flows, the stability criterion is not known, at the present time. Reshotko et al. (ref. 2) recommend for 2D and axisymmetric flows: $R_{e\theta,c} = R_{e\theta}/M_e = 150$, where M_e is the local edge Mach number.

This criterion is used to determine the beginning of transition, i.e., the location of minimum heat transfer level. In the PTM model, the growth of P_k can lag after being triggered by the stability criterion, therefore, $R_{e\theta,c}$ may need to be smaller than 150. In addition, it would be desirable to include in the PTM stability criterion the variation of TUE. This variation will be accurately included when more hypersonic transitional experimental data with measured noise level (to be converted into TUE level) will become available. For the present time, it is recommended to use $R_{e\theta,c}$ equal to 125 in the PTM technique. It should also be noted that the quantity $R_{e\theta}$ is not easy to compute accurately in particular for hypersonic flows over cones, because the edge of the boundary layer and therefore the momentum thickness, θ, is difficult to locate for these flows.

2.5 The law of the wall

The TURF code incorporates the capability of using the Law of the Wall boundary condition (LOW BC) with the high Reynolds number form of two-equation models. This type of boundary conditions is described in references 18 and 19. Its previous applications for fully turbulent flows with large separation (in particular, step flow) were quite successful regarding numerical efficiency. For example, without LOW BC, the step flow of ref. 19 could not be computed because for this flow the use of

integration to the wall boundary condition lead to prohibitively expensive computer runs. In the LOW BC, the wall shear stress is determined implicitly assuming that the computed velocity at the first cell center verifies a logarithmic profile. This assumption allows the use of a larger spacing in the direction normal to the wall corresponding to a dimensionless distance y^+ at least greater than 10.0, while with integration to the wall BC, y^+ must remain approximately less or equal to 1.0.

Numerical experimentations were made to investigate the feasibility of using LOW BC for transitional hypersonic flows over flat plates. The results of heat transfer were found sensitive to the wall spacing. For a dimensionless distance to the wall, y_+, of about 10, the peak of heat transfer was too high. For y_+ of about 100, it was too low. Therefore, by adjusting y^+, agreement with experiment could be reached! The inconveniency of the LOW BC is to use a velocity profile which is logarithmic, this is not true in the transition region. The behaviour of the velocity profile in the transition region of high speed flows is not well known at the present time. Much more theoretical work is needed to make the LOW BC applicable to transitional hypersonic flows. The use of integration to the wall with LRN two-equation models is recommended and was employed in this study.

3. RESULTS

Numerical simulations of hypersonic transitional flows over flat plates, sharp cones and blunt cones were performed with the TURF code and are reported in this section.

3.1 Flat plates.

3.1.1 Incompressible regime.

The implementation of the PTM technique in the TURF code was tested for flows over flat plates in the incompressible regime. Subsonic boundary conditions are used. The mesh size consist of 100 uniformly spaced points in the streamwise direction and 40 exponentially stretched points in the normal direction. Figures 5 and 6 compare skin friction results of Schmidt-Patankar with the TURF results, using the Jones-Launder model, without the PTM technique for free stream turbulence levels ranging from 1% to 6%. Figures 7 and 8 compare skin friction results of Schmidt-Patankar with the TURF results, using the Jones-Launder model and the PTM technique. Figure 6 shows that the TURF code with the Jones-Launder model without the PTM technique overpredicts the level of skin friction in the turbulence region for the highest levels of free-stream turbulence (TUE > 3%). In Figure 8, the peak of skin friction is smoothed by the PTM technique resulting in a spreading of the rise in skin friction and therefore of the transition zone. TURF results of Figures 6 and 8 agree with the Schmidt-Patankar results only satisfactorily. They could be improved with a finer mesh. Such computations require 300 CPU

seconds on the NAS CRAY, with a finer mesh computer time could be multiplied by 10 per case (i.e., per TUE value), this was outside the computer ressources of this project.

3.1.2 Richards flow.

In 1960, B.E. Richards (ref. 20) conducted an experimental investigation of natural transition and turbulent boundary layers on a cold flat plate in hypersonic flow in the Imperial College Gun Tunnel. The heat transfer equipment as described by Holden (ref. 21) was employed. Numerical simulations of this experiment were performed with the following test conditions:

angle of incidence= 0°,
free stream Mach number, M = 8.2,
stagnation temperature, T_0 = 775°K,
free stream unit Reynolds number, u_∞/ν_∞ per in. = 5.6×10^5,
model : a 1 foot long flat plate.
ratio of wall temperature to recovery temperature, T_w/T_r = 0.44.

The mesh consists of 100 cells uniformly spaced in the streamwise direction and 40 cells exponentially stretched in the normal direction. The first spacing in the normal direction is a function of the free stream Reynolds number.

The boundary conditions are:
- no slip on the flat plate surface, integration to the wall is applied. The wall temperature is imposed to $0.44*T_r$.
- inflow: all flow variables are fixed.
- outflow: all flow variables are extrapolated.

Implicit boundary conditions are used for the LHS operator.

Such mesh and boundary conditions are used for all the flow simulations reported here.

The beginning of transition is imposed to be 0.58 inches.

Figures 9 and 10 compare the results of turbulent kinetic energy, TKE, profiles along the flat plate without and with the PTM technique. In Figure 9, a sudden change of TKE is observed at transition onset, then the TKE profiles grow and flatten towards a fully turbulent (narrower) profiles. In Figure 10, the TKE profiles grow monotonically in the the transition region and converge toward a fully turbulent profile. The same qualitative behaviour was observed by Schmidt and Patankar for incompressible flows. Figures 11 and 12 show the comparisons of velocity profiles along the flat plate without and with the PTM technique. The profiles behave in the same qualitative way than the TKE profiles.

Figure 13 compare the results of TURF heat transfer with Richards experimental measurements, for a free stream turbulence level of 1%. In this Figure, we observe that when the transition model is not used, the Jones-Launder (J-L) model predicts

reasonably well the level of heat transfer peak but the transition zone is too narrow. When the J-L model with the PTM technique is used with A and B values as derived for incompressible flows, the predicted heat transfer is identical to the one predicted by the J-L model without the PTM technique. Hovewer, the PTM technique contributed to improve the rate of convergence of the computation. Such behaviour of the PTM solution is caused by a too large value of the PTM constant B. In Figure 13, results are shown for A and B divided by M. In this case, the peak of heat transfer is too low. When A is not modified and B divided by M^3, we observed a delay in the beginning of transition but the peak of heat transfer is still too low. In Figure 13, in the laminar regime, the computed heat transfer is too low. Various mesh spacings in the normal and streamwise direction were tested without any effect on the results. This too low level of heat transfer needs to be investigated, it could be caused by experimental or numerical errors, or to a physical aspect of the flow not modeled by the numerical simulation.

In Figure 14, the effect of varying TUE (TUE=2%) was investigated for the cases where the PTM constants A and B are both divided by M, and for the case where B alone is divided by M^3. In the first case, the heat transfer has increased but the transition zone is narrower than for the case with TUE=1%, the second case shows some improvement. In all cases, the PTM technique does not predict the experimentally observed slow rise of heat transfer starting upstream in the laminar regime.

3.1.3 Keener flow.

Starting in the early sixties, Earl Keener and Thomas Polek (ref. 22) performed a series of wind tunnel experiments at Ames Research Center to measure heat transfer on flat plates for hypersonic flows. The results although not published were made available for this study.

In this experiment, air is heated to temperatures ranging about 670 to 1170 degrees Kelvins. This is necessary to prevent air condensation that will occur otherwise, causing a transitional two-phase flow. The test section pressure is about 13 pounds per square feet. The gas is assumed perfect. The molecular viscosity is determined as a function of temperature by the Sutherland law.

The flow conditions are:

free stream Mach number, M = 7.4,
free stream temperature = 173° Rankines,
wall temperature = 547° Rankines, corresponding to a ratio of wall to adiabatic wall temperature of 0.3.
The flat plate length is 1 meter. TUE was set to 1%.

Figure 15 shows results of heat transfer variation along the flat plate. The transition onset is imposed and equal to 50 cm. In the fully laminar case for a free stream Reynolds number, Re,

per meter of 1,890,000, agreement between experimental and computation is excellent, indicating that the computation is numerically accurate regarding the mesh size and assumptions (Sutherland law, perfect gas ...). For higher Reynolds numbers, in the laminar regime, the computed heat transfer is too low. The J-L model without and with the PTM technique (A and B equal to their "incompressible" values) was applied and provided the same results. In Figure 15, results are also shown with the J-L model and the PTM technique for cases where A and B are divided by M, and where B alone is divided by M^3. In this case, the best agreement is obtained when A and B are divided by M.

3.2 Sharp cones

3.2.1 Martellucci experiment, sharp cone.

Heat transfer data on a 7.2° half-angle cone have been obtained by Martellucci et al. (ref. 23).

Figure 16 shows comparisons of calculated and measured Stanton number for the following flow conditions:

free stream Mach number = 7.99,
free stream temperature = 68.59°K,
free stream Reynolds number per foot = 3.79×10^6,
T_w/T_r = 0.3. TUE is set to 1%. The onset of transition is imposed.

Figure 16 displays four computed curves of Stanton number:

curve 1: J-L model without PTM technique.
curve 2: J-L model with PTM technique (A and B set to their incompressible values),
curve 3: J-L model with PTM technique, A divided by M, B divided by M^2,
curve 4: J-L model with PTM technique, A divided by M, B divided by M^3.

Results for this flow were inconclusive, curve 4 shows a spreading of the transition zone but no peak of heat transfer. In the four cases, agreement between computations and experimental measurements is not very good and the above sets of A and B values for curves 3 and 4 were not used anymore.

3.2.2 Muir and Trujillo experiment, sharp cone.

Muir and Trujillo (ref. 24) performed a series of experiments to study boundary layer transition on an 8 degree half-angle cone. The experiments took place in the U.S. Naval Ordnance Laboratory's Hypersonic Wind Tunnel. Effects of nose bluntness were investigated. This experiment was simulated first for the sharp cone model. The nominal wall to recovery temperature ratio is 0.6.

The free stream turbulence level is set to 2 %. The onset of transition is imposed.

The following four test conditions were applied:

cases	M	$u_\infty/\nu_\infty x10^{-6}$/ft	T_o degrees Rankines
1	5.9	3.	1092.
2	6.	9.7	1127.
3	6.	17.	1162.
4	6.	23.6	1162.

T_o is the stagnation temperature.

Figure 17 compares the results of Stanton number versus Reynolds number based on distance along the cone surface, for the four free stream Reynolds numbers given above. The J-L model is used without transition model. The width of the transition zone is very narrow in all cases.

Figure 18 shows the same kind of comparisons when the J-L model is used with the PTM technique. The PTM parameter B is divided by M^3, A is unchanged. The computation predicts the width of the transition zone very well. In the laminar region, the discrepancy between the numerical results is attributed to a coarse first cell spacing from the wall.

Figure 19 shows another set of comparisons between computed and measured Stanton number. In this case, the J-L model is used with a modified production term. The production term of the k and ϵ equations in the J-L model is modified by the intermittency factor (formula 78, p. 20 of Adams report, ref. 25). The numerical results predict fairly well the extent of the transition zone, but the peak of Stanton number is smeared, and for this reason the PTM technique was prefered.

Figure 20 shows the variation of Reynolds number based on momentum thickness versus the Reynolds number based on distance along the cone axis. It is observed that the onset of transition occurs at $R_{e\theta}$ = 700 for Re/ft = 3,000,000 and at $R_{e\theta}$ = 900 for the other values of Re/ft. For this flow, the edge Mach number is 5.24. If we were to use a stability criterion the effect of TUE would need be incorporated in the criterion.

3.3 Blunt cones.

Numerical predictions of heat transfer were performed for blunt cones by Martellucci et al. (ref. 23) and Muir and Trujillo (ref. 24). The numerical simulations of some of these experiments are reported below.

3.3.1 Martellucci experiment, blunt cone.

The test conditions are:

cone half-angle = 7.2°,
free stream Reynolds number per foot = 3.79×10^6,
ratio of nose radius over base radius, $R_N/R_B = 0.02$,
free stream Mach number = 8.
TUE = 1%.

Figure 21 presents an enlargement of the nose region mesh. Figure 22 shows typical density contours. Figures 23 and 24 show some entropy contours and an enlargement of the entropy contours in the nose region.

Figure 25 compares the results of computed Stanton number versus streamwise distance with Martellucci et al. experimental measurements. The J-L model is used in the four cases:

1. no transition used.
2. PTM technique used with A and B equal to their incompressible values.
3. PTM technique used with A unchanged and B divided by M^3.
4. PTM technique used with A unchanged and B divided by M^4.

In Figure 25, curve 4 seems to provide the best predictions.

3.3.2 Muir and Trujillo experiment, blunt cone.

Muir and Trujillo experiment for a blunt cone was simulated for the four test conditions mentioned above for a sharp cone in Section 3.2.2. The model is a blunt cone of nose radius equal to 0.1 inches.

The transition onset is imposed.

TUE is equal to 2%.

Figure 26 shows results of Stanton number versus Reynolds number based on distance along the cone surface, when the J-L model is used without the PTM technique. The width of the transition zone is too narrow.

Figure 27 shows results of Stanton number versus Reynolds number based on distance along the cone surface, when the J-L model is used with the PTM technique and with B divided by M^3, A unchanged. In this case, the agreement between computed results and experimental measurements is very good with respect to the prediction of the extent of the transition zone and the peak level of Stanton number. In the laminar regime, the discrepancy between the computed results is caused by a too coarse first cell spacing.

4. CONCLUSIONS.

A new transition model was tested for hypersonic transitional flows over flat plates, sharp and blunt cones. The transition model was first developed for incompressible flows, the effect of free stream turbulence levels is built in the model. In the applications of this model to hypersonic transitional flow, the model constants had to be modified. Attempts were made to introduce a free stream Mach number effect. In some instances, the computed results agree very well with experimental measurements. The level of free stream turbulence (or noise) is seen to significantly influence the results. In the experiments simulated here, the free stream noise level was not measured making difficult to relate the TUE value to the noise level. However, the best computed results were obtained for the simulation of the Muir and Trujillo experiment for TUE=2%, which, from our crude conversion analysis of TUE into noise (or vice versa), corresponds to a free-stream rms pressure fluctuations divided by mean static pressure (or noise level) of 4%. From Figure 4, at Mach 6, the noise level in wind tunnels can vary from 1% to 4%, which is in satisfactory agreement with the value used in the computations.

The transition model employs a stability criterion to determine the transition onset. The Bushnell stability criterion was found to perform approximately well, but this criterion needs to be refined. It is necessary to introduce in the stability criterion the effect of free stream turbulence level (or noise). An additional contract would be required to pursue further investigations on this important aspect of transition modeling.

The reported results are encouraging and the PTM transition model shows potential of becoming a predictive tool for hypersonic transitional flows. More work is required to compare computations and experimental measurements for a large variety of hypersonic transitional flows over cones, which will establish the universality of the model.

5. REFERENCES

1. "Special Course on Stability and Transition of Laminar Flow," AGARD Report No. 709, North Atlantic Treaty Organization, March 1984.

2. Reshotko, E., Bushnell, D.M., and Cassidy, M.D., "Report of the Task Force for Boundary Layer Transition," NASP Technical Memorandum 1007, NASA Langley Research Center, April 1987.

3. Pate, S.R., "Effects of Wind Tunnel Disturbances on Boundary-Layer Transition with Emphasis on Radiated Noise: A Review," AIAA Paper 80=0431, 11th Aerodynamic Testing Conference, Colorado Springs, Colorado/March 18-20, 1980.

4. Kovasnay, L.S.G., "Turbulence in Supersonic Flow," Journal of the Aeronautical Sciences, Vol. 20, No. 10, October 1953, pp. 657-674.

5. Stetson, K.F., "Laminar Boundary Layer Stability Experiment on a Cone at Mach 8, Part 4: On Unit Reynolds Number and Environmental Effects," AIAA paper No. 86-1087, AIAA/ASME 4th Fluid Mechanics, Plasma Dynamics and Lasers Conference, May 12-14, 1986, Atlanta, GA.

6. Beckwith, I.E., "Development of a High Reynolds Number Quiet Tunnel for Transition Research," AIAA Journal Vol. 13, No. 3, pp. 300-306.

7. Dougherty, N.S., Jr. and Fisher, D.F., "Boundary-Layer Transition on a 10-Degree Cone: Wind Tunnel/Flight Data Correlation," AIAA Paper No. 80-0154, AIAA 18th Aerospace Sciences Meeting, January 1980.

8. Schmidt, R.C., and Patankar, S.V., "Two-Equation Low-Reynolds-Number Turbulence Modeling of Transitional Boundary Layer Flows Characteristic of Gas Turbine Blades," NASA Contractor Report 4145, 1988.

9. Coakley, T.J., "Implicit Upwind Methods for the Compressible Navier-Stokes Equations," AIAA Journal, Vol. 23, No. 3, March 1985, p. 374.

10. Coakley, T.J., "Turbulence Modeling Methods for the Compressible Navier-Stokes Equations," AIAA Paper 83-1693, 1983.

11. Yoon, S. and Jameson, A., "An LU-SSOR Scheme for the Euler and Navier-Stokes Equations," AIAA Paper 87-0600, Jan. 1987.

12. Chien, K.-Y., "Predictions of Channel and Boundary-Layer Flows with a Low-Reynolds Number Turbulence Model," AIAA Journal, Vol. 20, No. 1, pp. 33-38, 1982.

13. Jones, W.P., and Launder, B.E., "The Prediction of Laminarization with a Two-equation Model of Turbulence," Int. J. of Heat and Mass Transfer, Vol. 15, pp. 301-314, 1972.

14. Lam, C.K.G. and Bremhorst, K., "A Modified Form of the k-ϵ Model for predicting Wall Turbulence," J. of Fluids Engineering, Vol. 103, pp. 456-460, Sept. 1981.

15. Abu-Ghannam, B.J., and Shaw, R., "Natural Transition of Boundary Layers - The effects of Turbulence Pressure Gradient, and Flow History," Journal Mechanical Engineering Science, Vol. 22, No. 5, 1980.

16. Laufer, J., Williams, J.E.F. and Childress, S., "Mechanism of Noise Generation in the Turbulent Boundary Layer," AGARDograph 90, November 1964,

17. Shamroth, S.J. and MacDonald, H., "Assessment of a Transition Boundary-Layer Theory at Low Hypersonic Mach Numbers," NASA CR-2131, Langley.

18. Champney, J.M., "Incompressible Viscous Flow Simulations of the NFAC Wind Tunnel," NASA Contractor Report 177431, June 1986.

19. Champney, J., "Computations of Separated Flows with Two-equation Models," ATM-FR-21-023, September 1988, accepted for presentation at the next Propulsion Conference to be held at Monterey, CA. July 1989. (co-authors: T.J. Coakley, N.N. Mansour)

20. Richards, B.E. "Transition and Turbulent Boundary Layers on a Cold Flat Plate in Hypersonic Flow," The Aeronautical Quarterly, Vol. XVIII, August 1967, pp. 237-258.

21. Holden, M.S., "Heat Transfer in Separated Flow," PhD thesis, University of London, 1963.

22. Keener, E.R. and Polek, T.E., "Hypersonic Boundary Layer Transition on a Nonadiabatic Flat Plate," Unpublished 1974.

23. Martelluci, A., Chaump, L., Rogers, D. and Smith, D., "Experimental Determination of the Aeroacoustic Environment About a Slender Cone," AIAA Journal Vol. 11, No. 5, pp 635-642, May 1973.

24. Muir J.F. and Trujillo A.A., "Experimental Investigation of the Effects of Nose Bluntness, Free-stream Unit Reynolds Number, and Angle of Attack on Cone Boundary Layer Transition at a Mach Number of 6," AIAA Paper No. 72-216, AIAA 10th Aerospace Sciences Meeting, San Diego, CA., Jan. 17-19, 1972.

25. Adams, J.C., "Eddy Viscosity Intermittency Factor Approach to Numerical Calculation of Transitional Heating on Sharp Cones in Hypersonic Flow," AEDC-TR-71-235, December 1971.

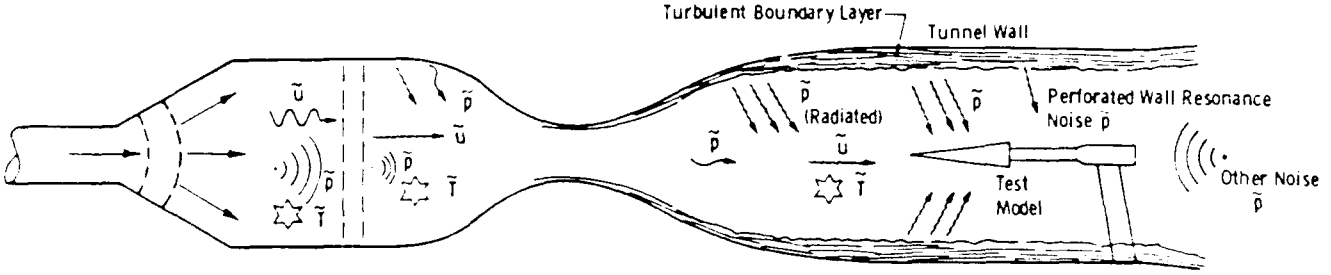

Vorticity (Turbulence - Velocity Fluctuations), $\tilde{u}$
Acoustic Sound (Pressure Fluctuations), $\tilde{p}$
Entropy Fluctuations (Temperature Spottyness), $\tilde{T}$

Mach Number Range	Type Disturbance		Effect on Transition
Subsonic $M_\infty \leq 0.6$	Velocity Fluctuations,	$\tilde{u}$	• Usually Dominant
	Acoustic Noise,	$\tilde{p}$	• Can be Dominant
	Temperature Fluctuations,	$\tilde{T}$	Negligible
Transonic $0.6 \leq M_\infty \leq 1.3$	Velocity Fluctuations,	$\tilde{u}$	• Can be Dominant
	Acoustic Noise,	$\tilde{p}$	• Usually Dominant
	Temperature Fluctuations,	$\tilde{T}$	Negligible
Supersonic $1.3 \leq M_\infty \leq 6$	Velocity Fluctuations,	$\tilde{u}$	Usually Negligible
	Radiated Noise,	$\tilde{p}$	• Usually Dominant
	Temperature Fluctuations	$\tilde{T}$	Usually Negligible
Hypersonic $6 \leq M_\infty \leq 15$	Velocity Fluctuations,	$\tilde{u}$	Usually Negligible
	Radiated Noise,	$\tilde{p}$	• Usually Dominant
	Temperature Fluctuations,	$\tilde{T}$	Could be Significant

Figure 1. Flow disturbances in Wind Tunnels.

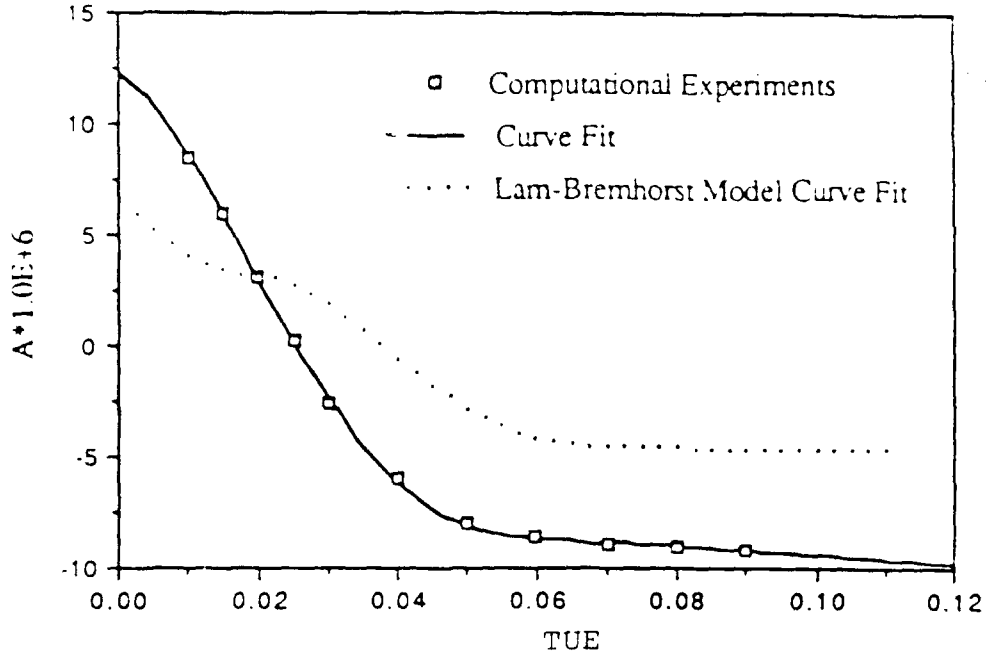

Figure 2. Variation of "A" with free-stream turbulence intensity for the Jones-Launder model.

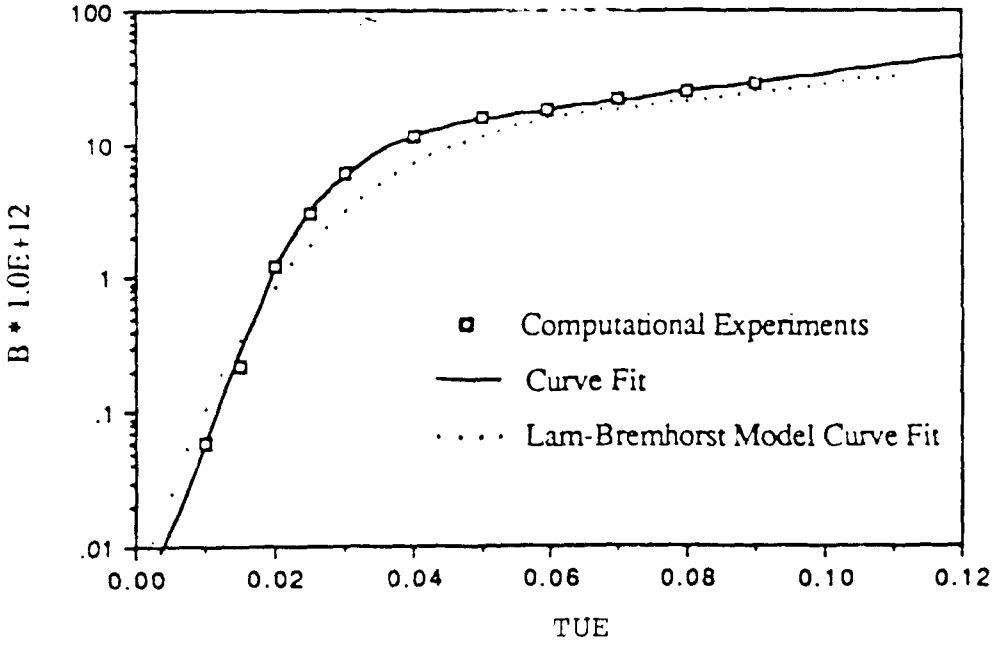

Figure 3. Variation of "B" with free-stream turbulence intensity for the Jones-Launder model.

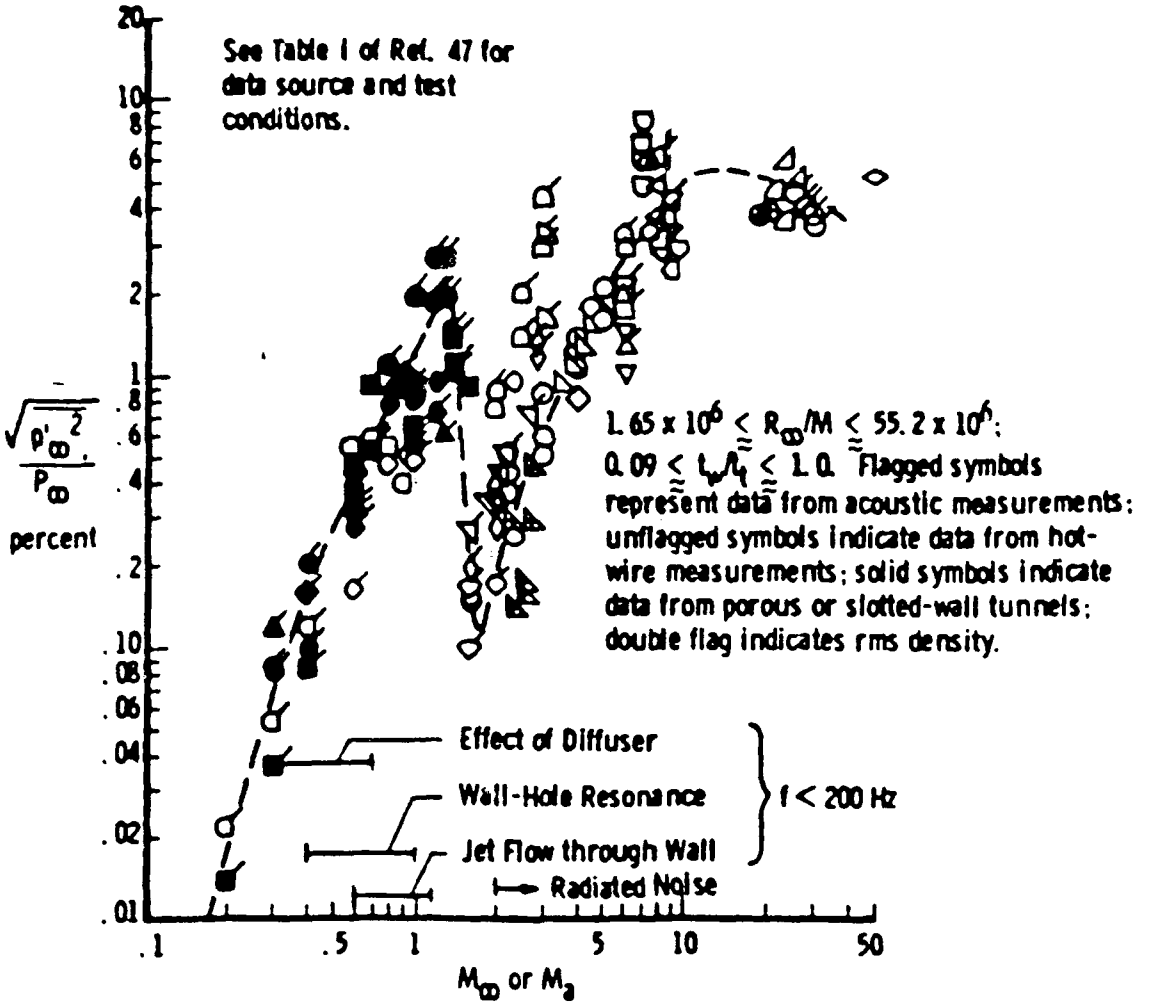

Figure 4. Free-stream rms pressure fluctuations divided by mean static pressure versus Mach number.

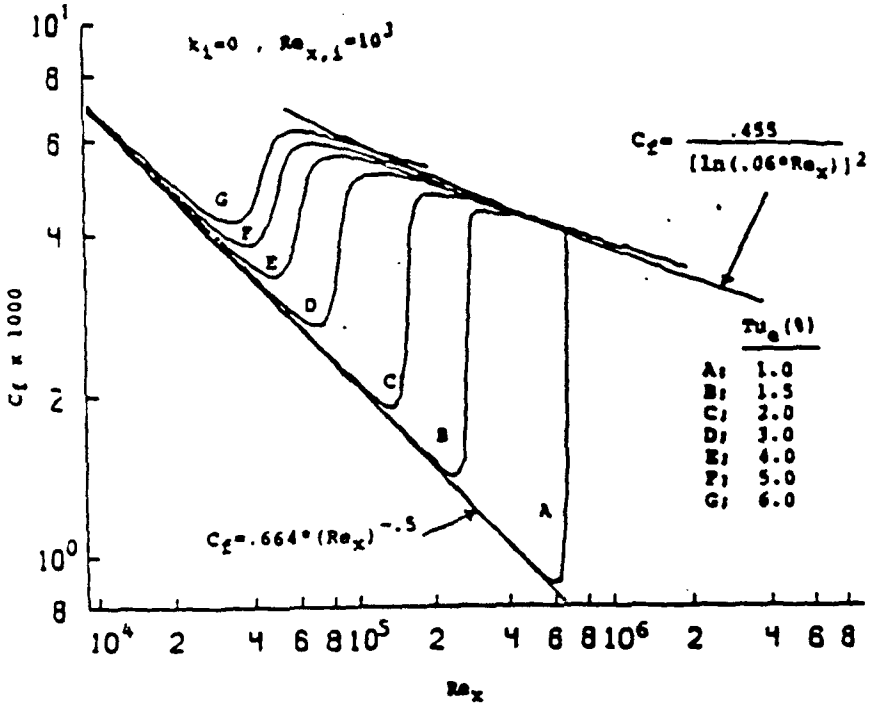

Figure 5. Skin friction versus Reynolds number based on streamwise distance, computed by Schmidt and Patankar with the Jones-Launder model without the PTM technique.

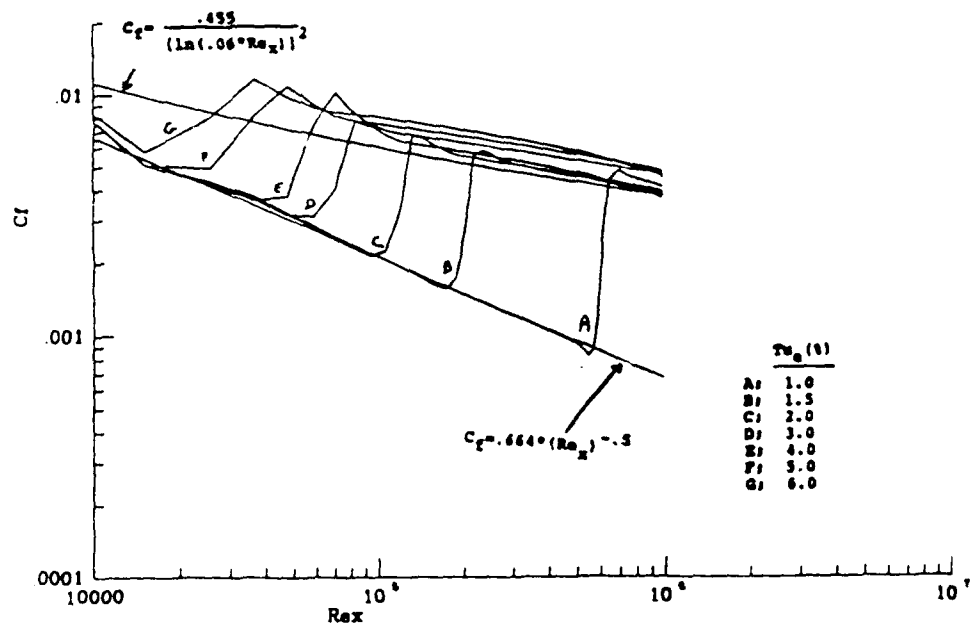

Figure 6. TURF computed skin friction versus Reynolds number based on streamwise distance, with the Jones-Launder model and without the PTM technique.

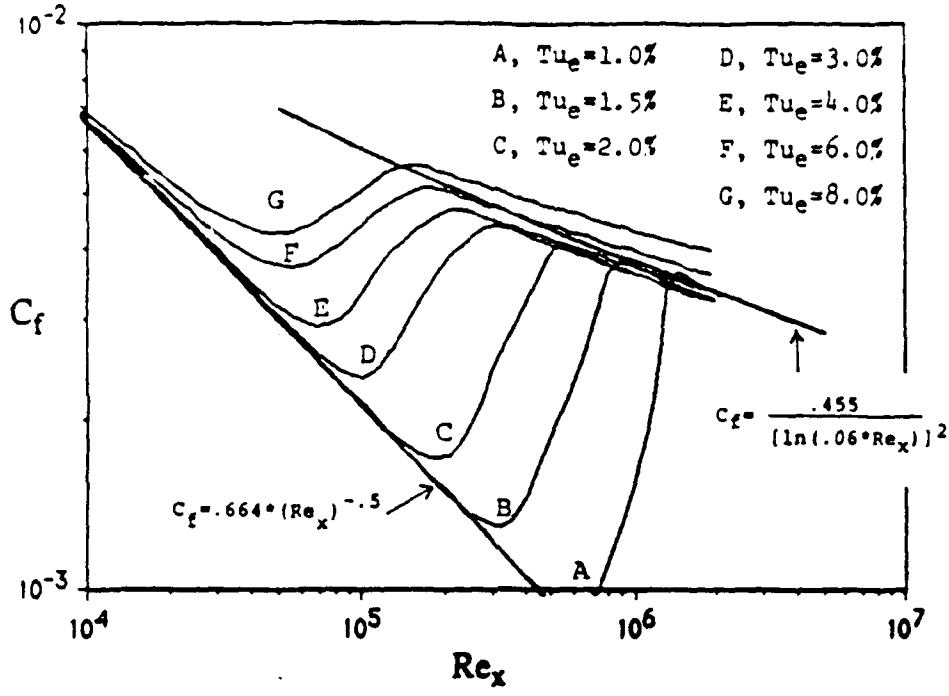

Figure 7. Skin friction results of Schmidt and Patankar obtained with the Jones-Launder model and the PTM technique.

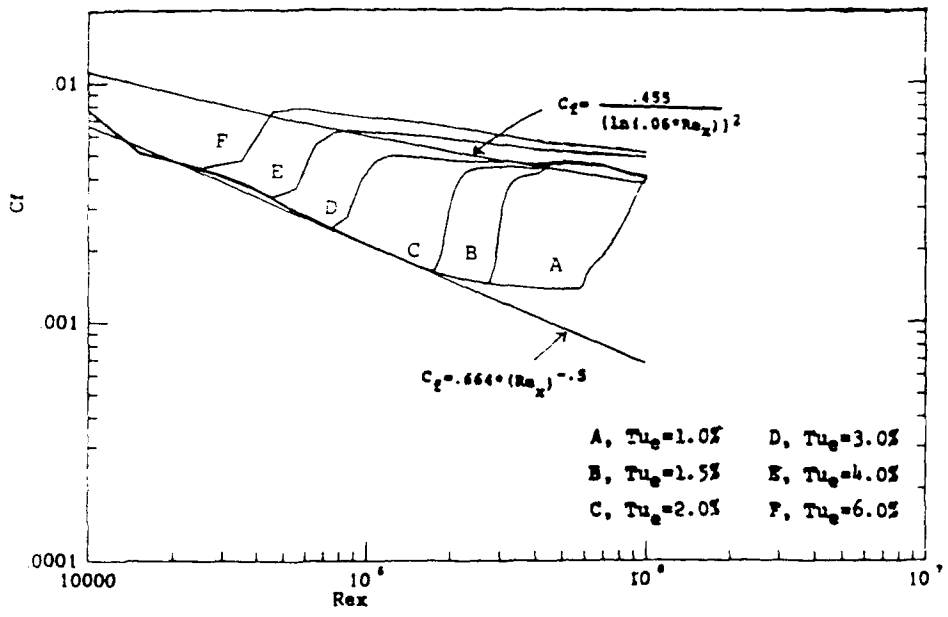

Figure 8. TURF computed skin friction with the Jones-Launder model and the PTM technique.

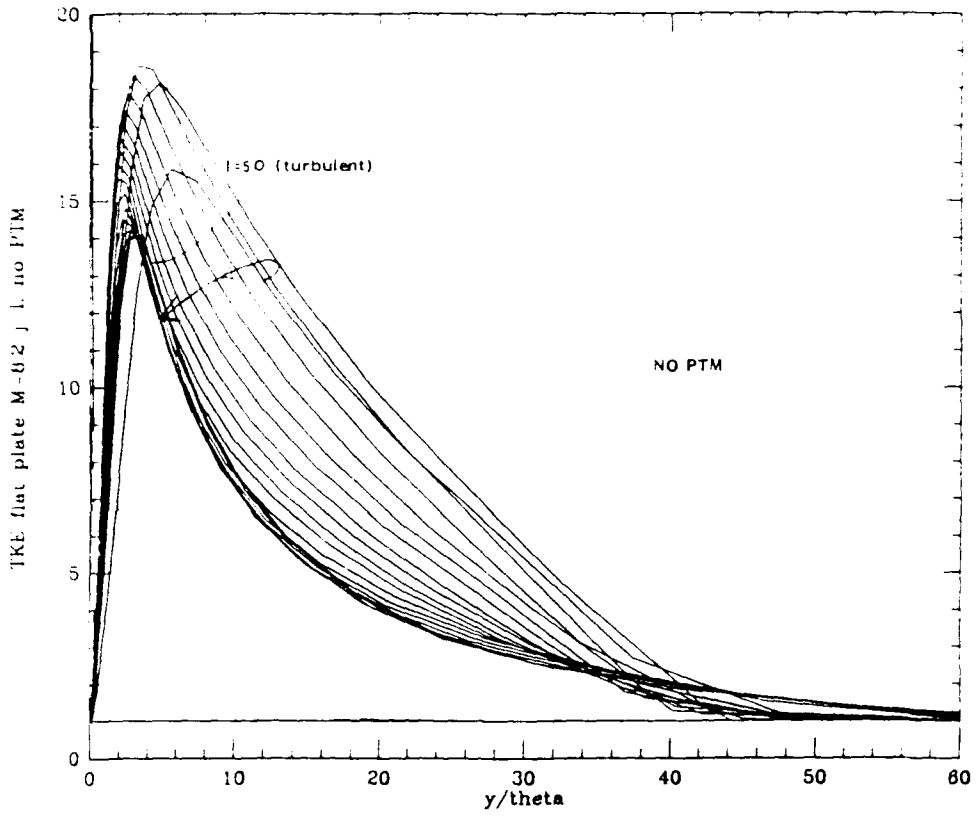

Figure 9. Profiles of turbulent kinetic energy for a flat plate flow at Mach 8.2 - No PTM used.

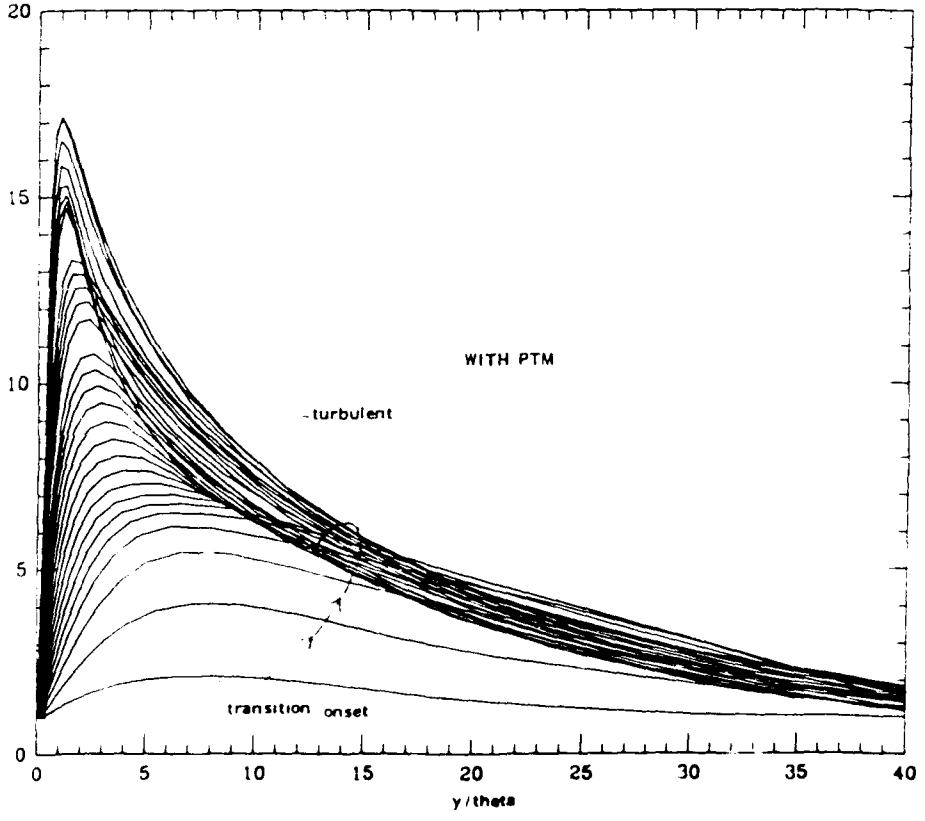

Figure 10. Profiles of turbulent kinetic energy for a flat plate flow at Mach 8.2 - PTM used.

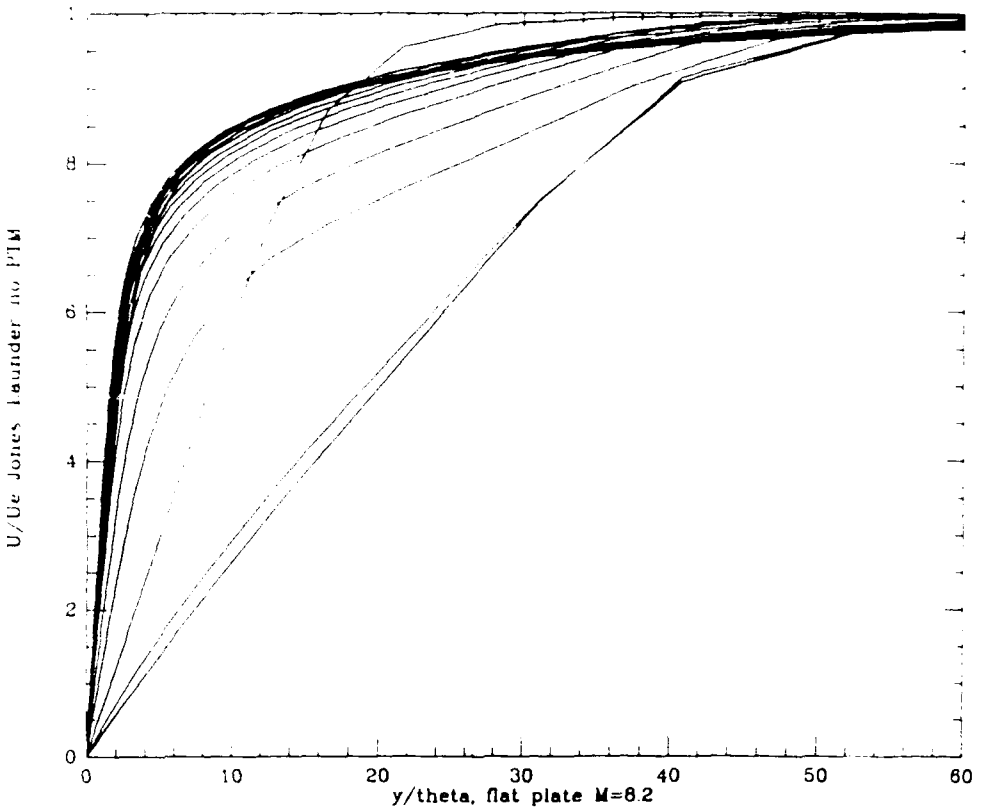

Figure 11. Velocity profiles along flat plate, M=8.2, No PTM.

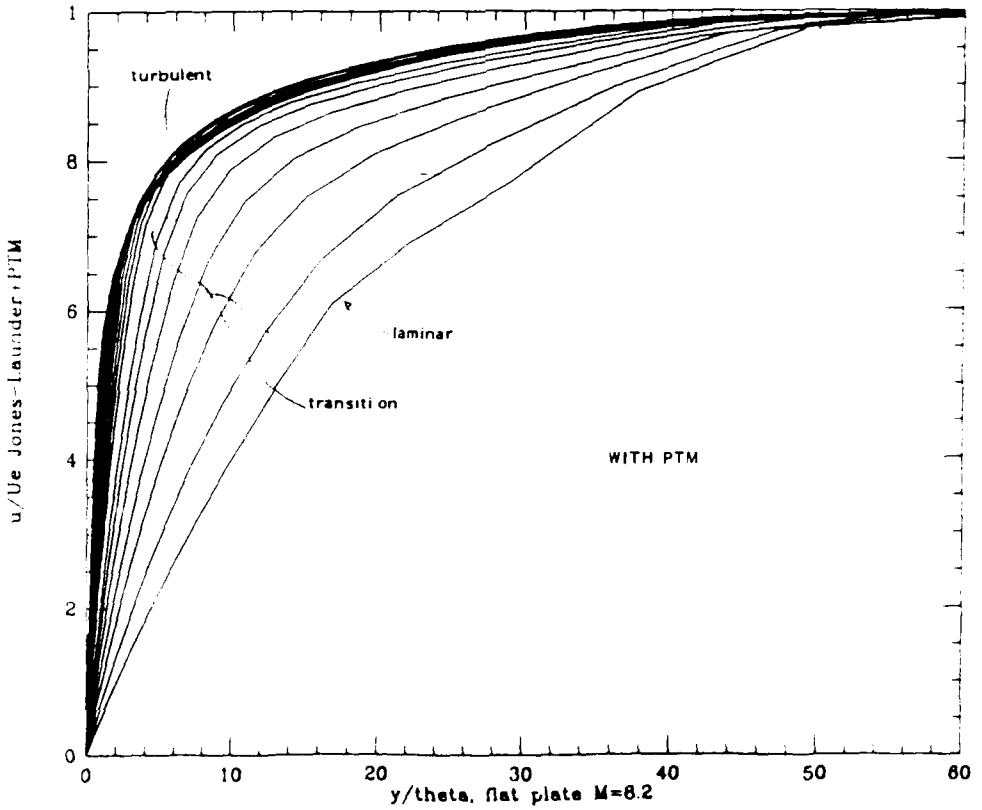

Figure 12. Velocity profiles along flat plate, M=8.2, PTM used.

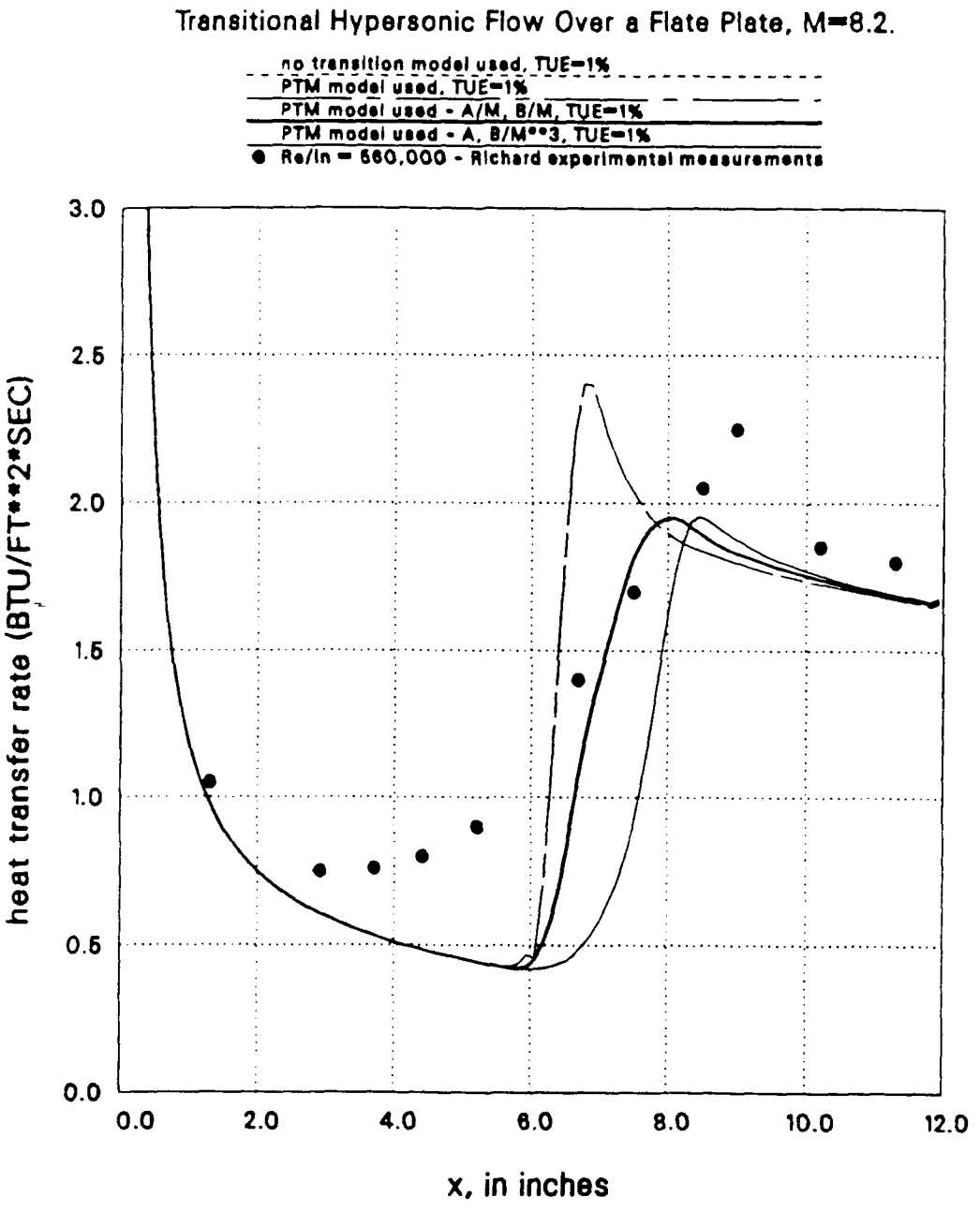

Figure 13. Comparisons between computed and experimental heat transfer, R_e/in. = 560,000.

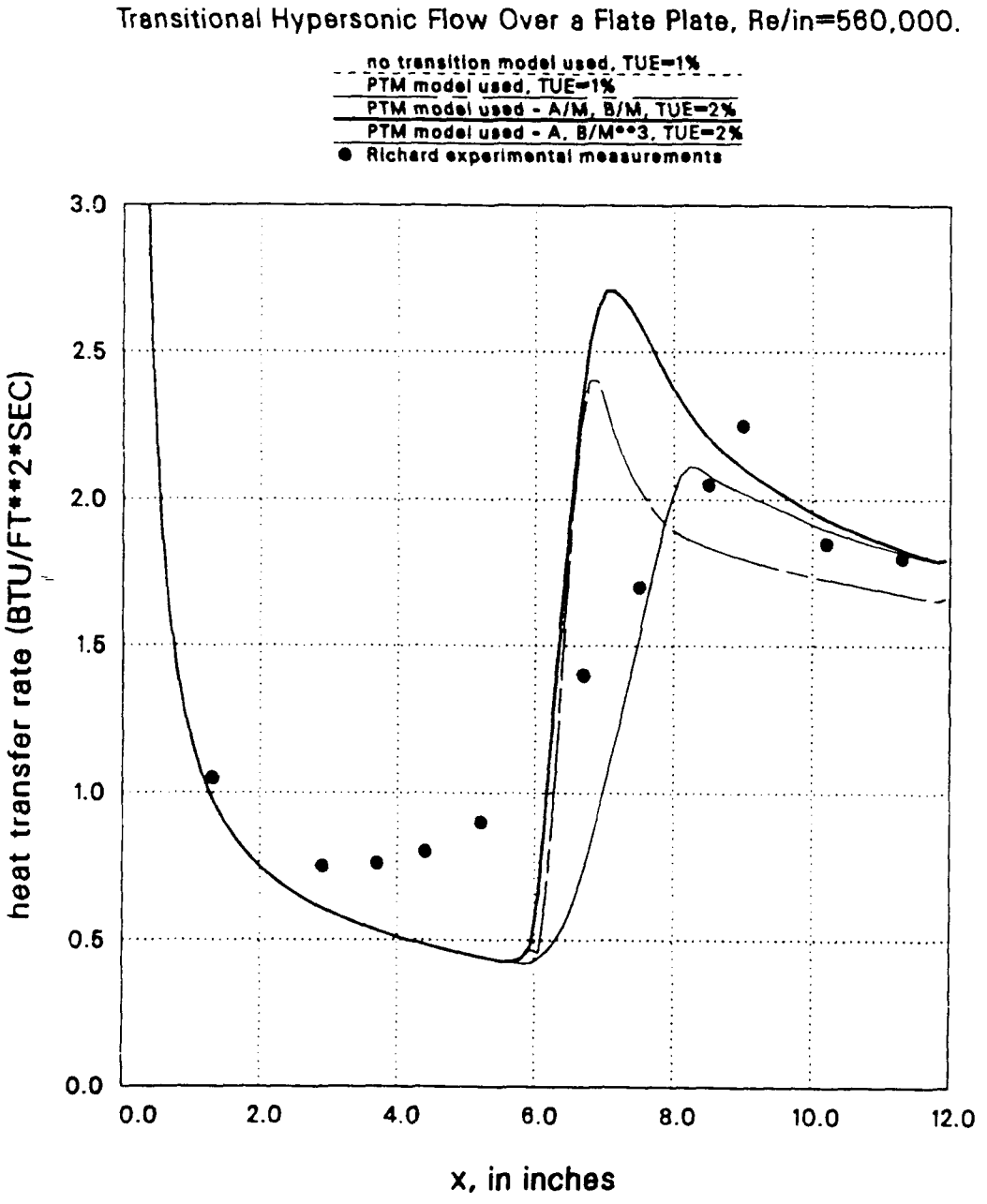

Figure 14. Comparisons between computed and experimental heat transfer, M = 8.2, showing TUE effect.

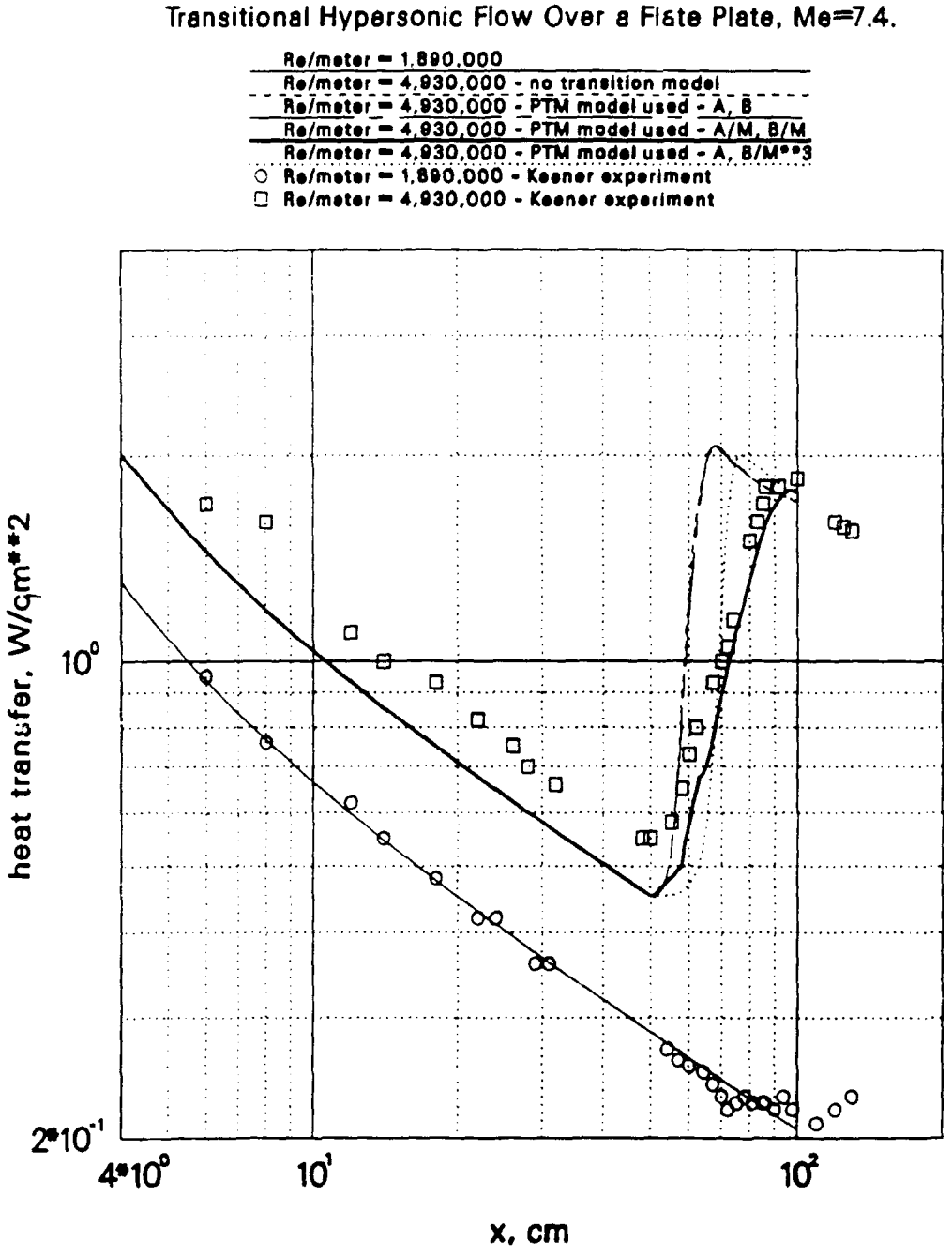

Figure 15. Comparisons between computed and experimental heat transfer.

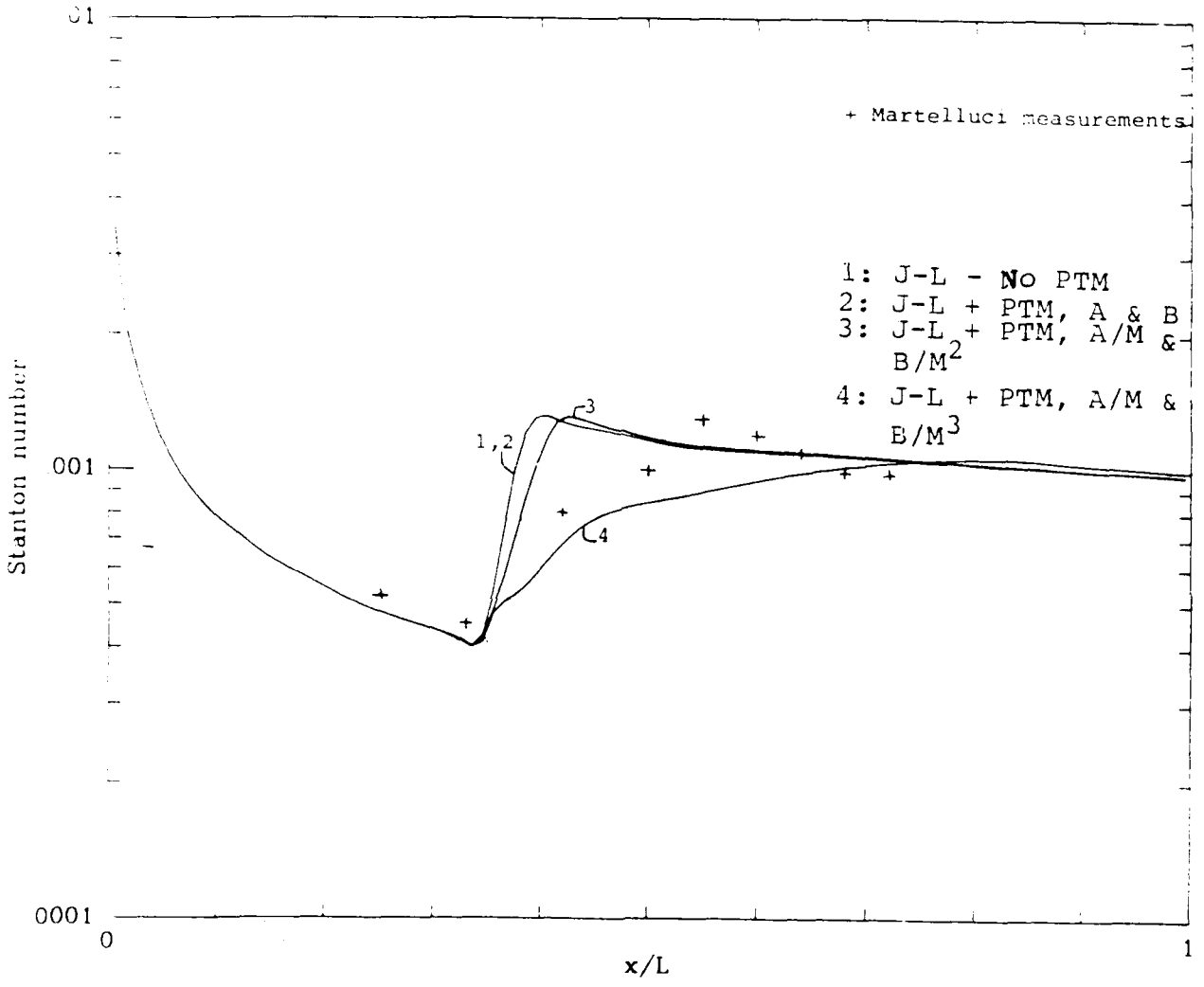

Figure 16. Comparisons of computed and measured Stanton number for flow over a sharp cone at Mach 8.

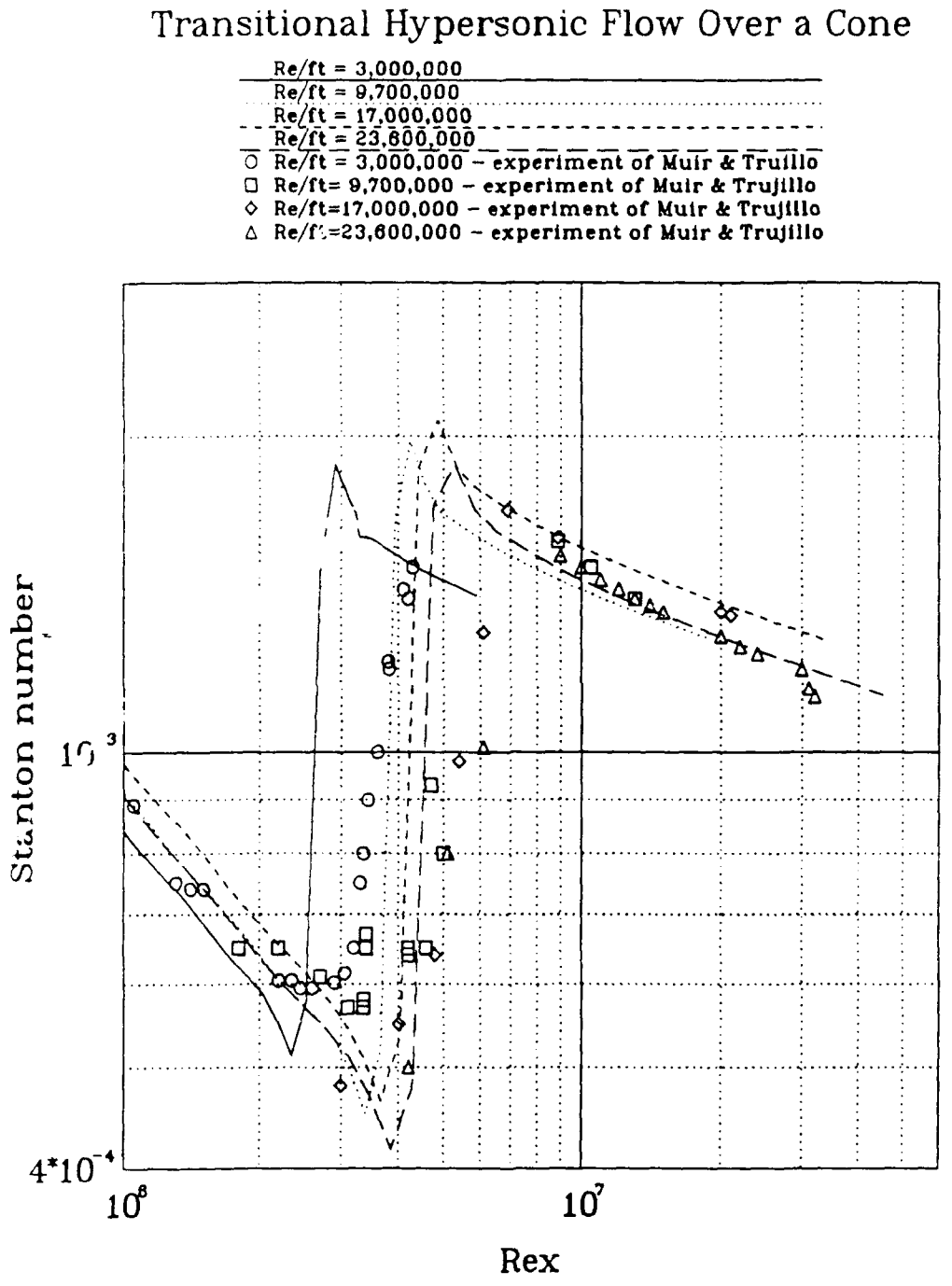

Figure 17. Streamwise variation of Stanton number, no transition model used.

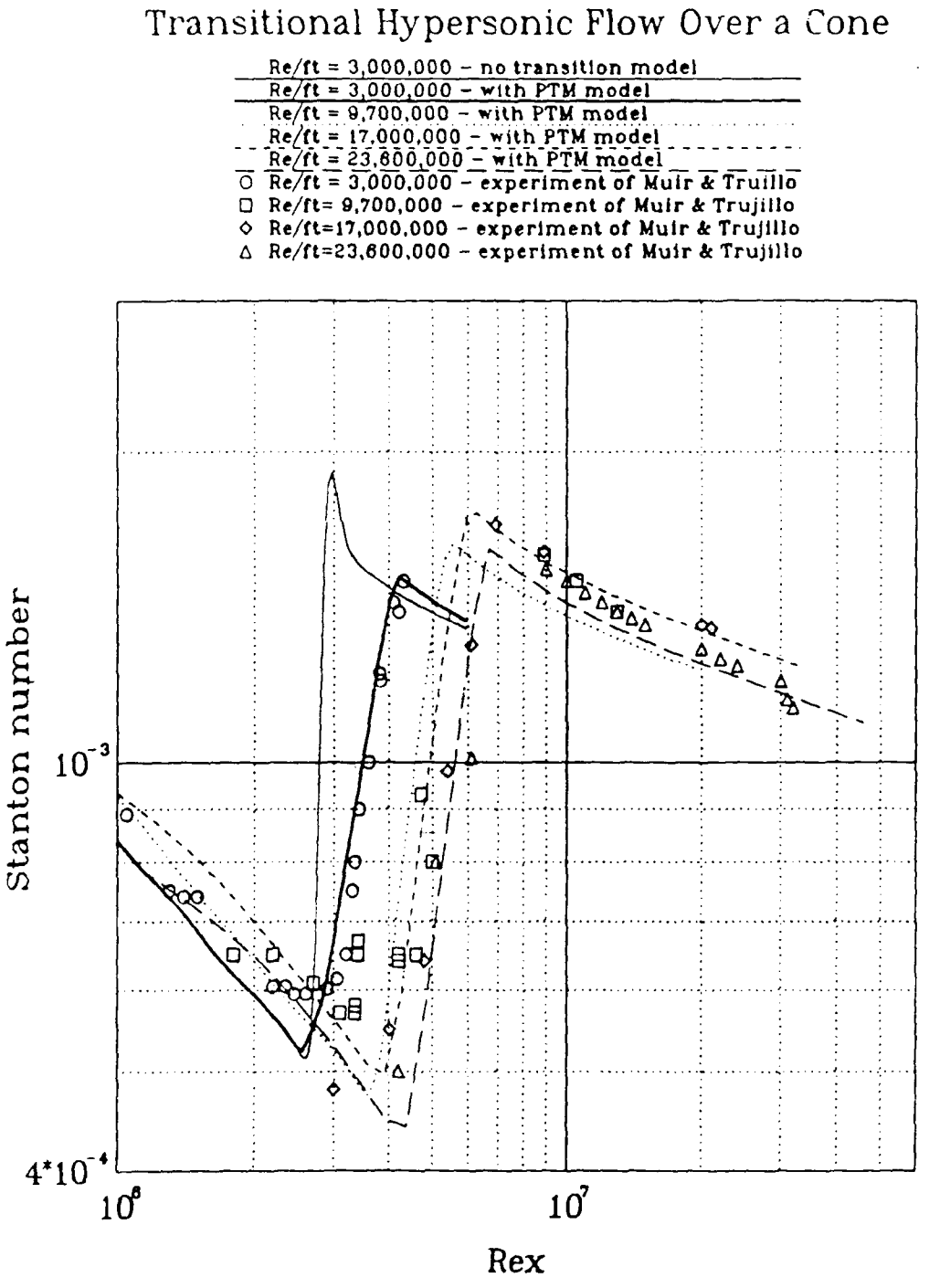

Figure 18. Comparisons between computed Stanton number and experimental measurements. The PTM technique is used.

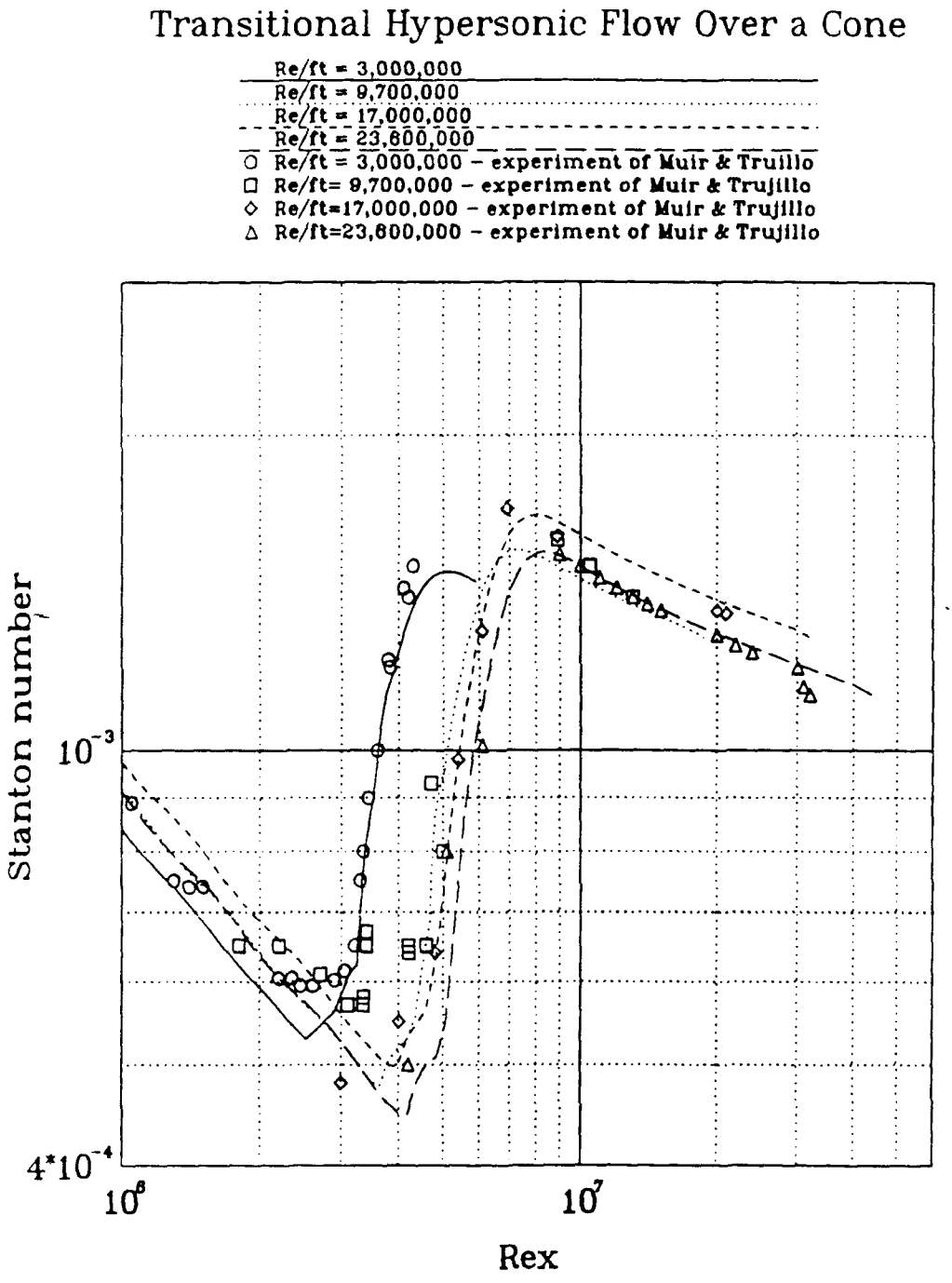

Figure 19. Streamwise variation of Stanton number, the intermittency factor approach of Adams is used.

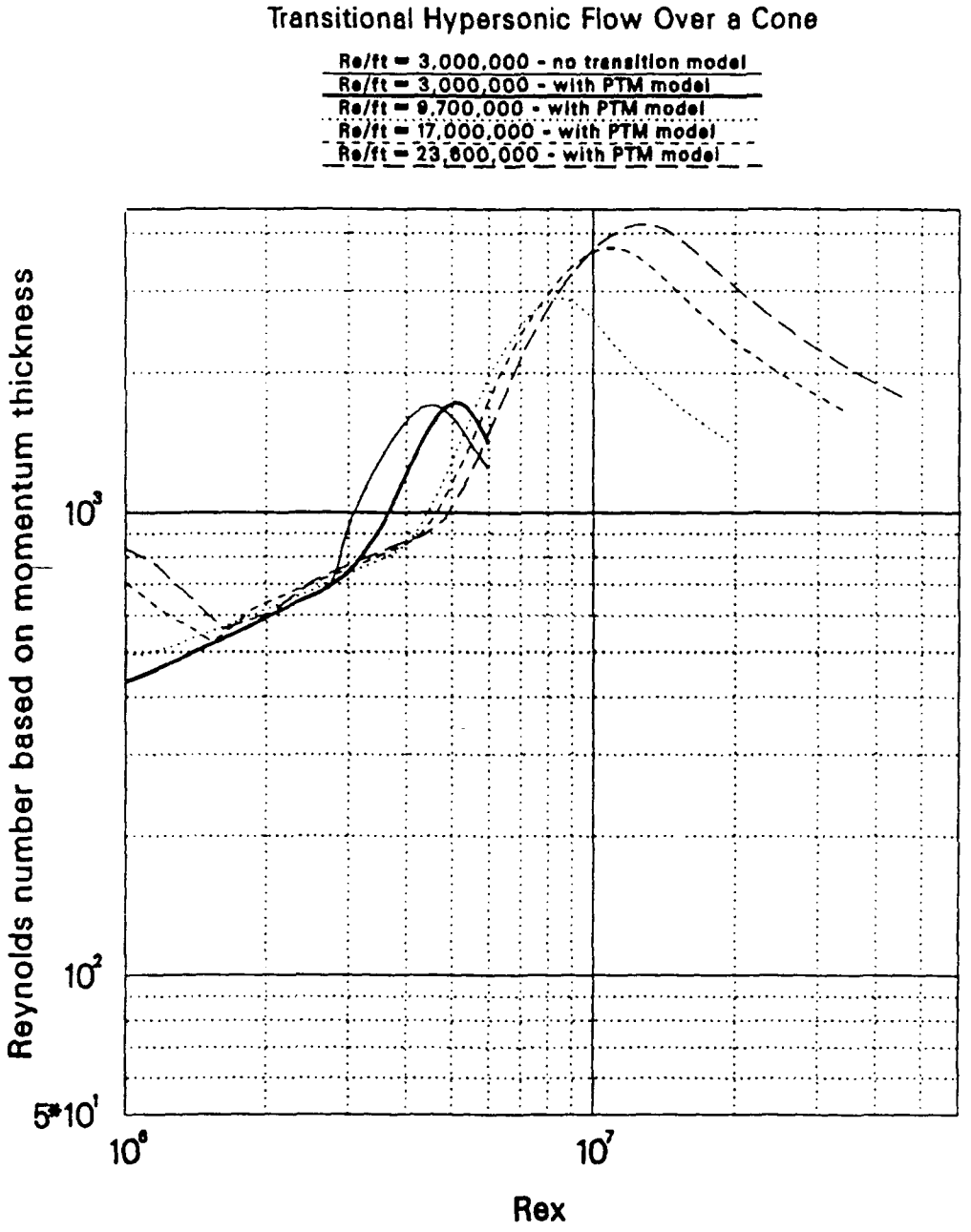

Figure 20. Variation of Reynolds number based on momentum thickness versus R_{ex}.

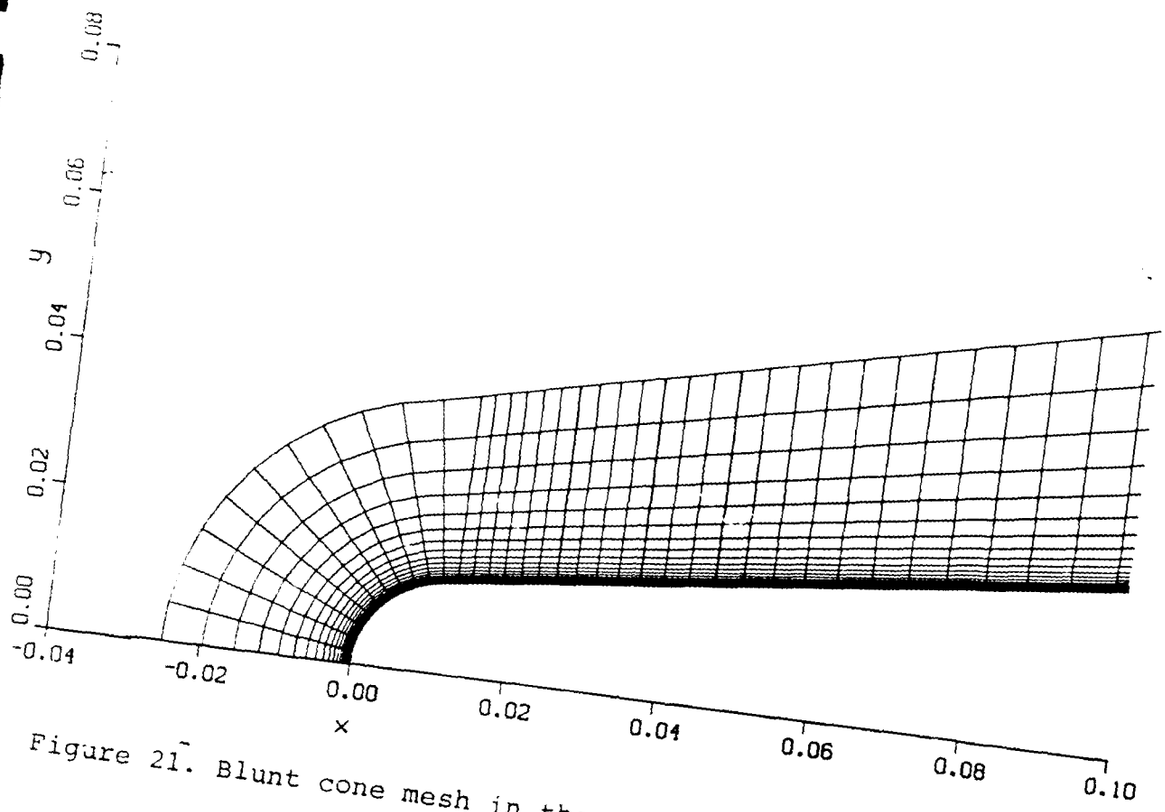

Figure 21. Blunt cone mesh in the nose region.

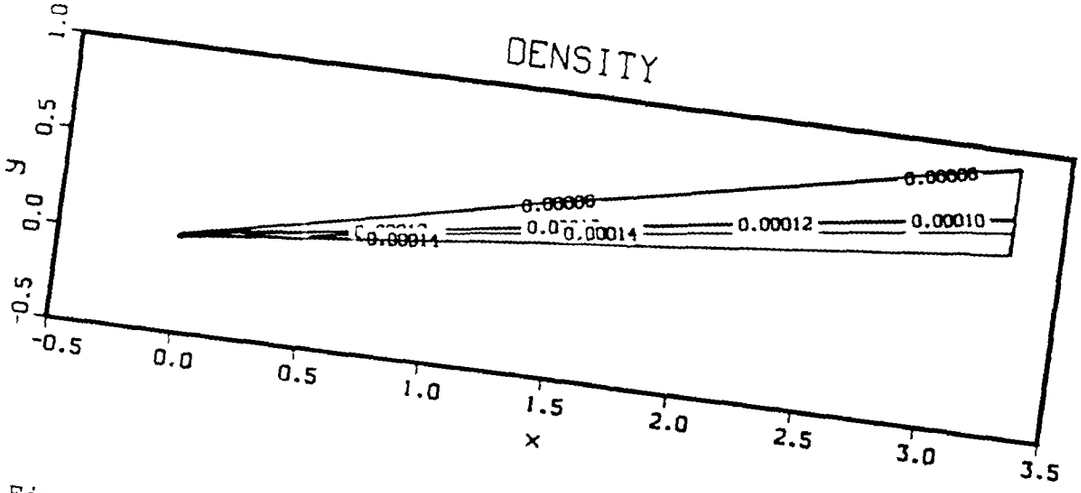

Figure 22. Density contours for the blunt cone, at Mach 8.

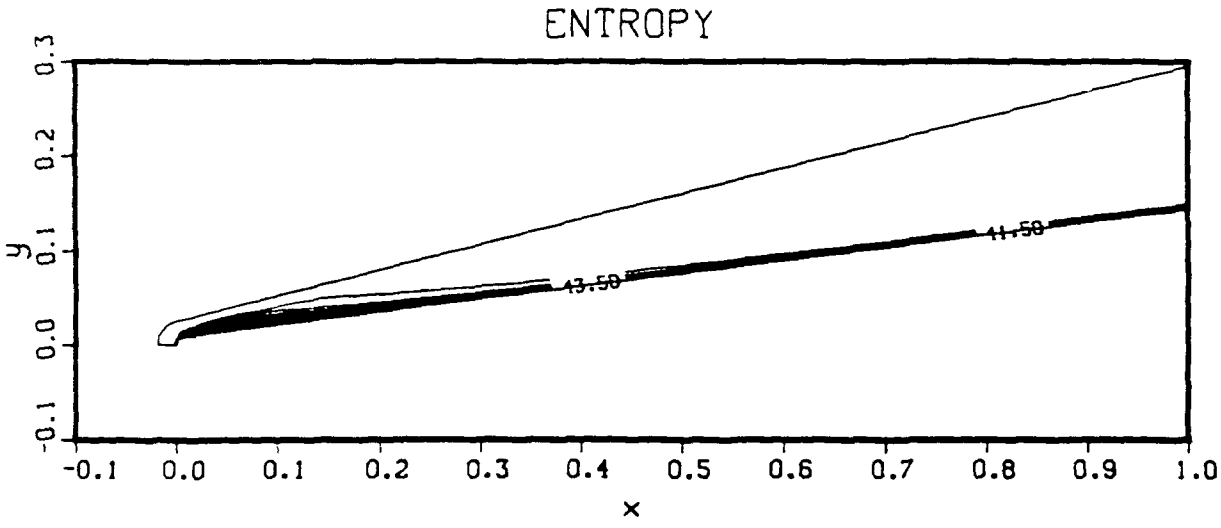

Figure 23. Entropy contours, blunt cone at Mach 8.

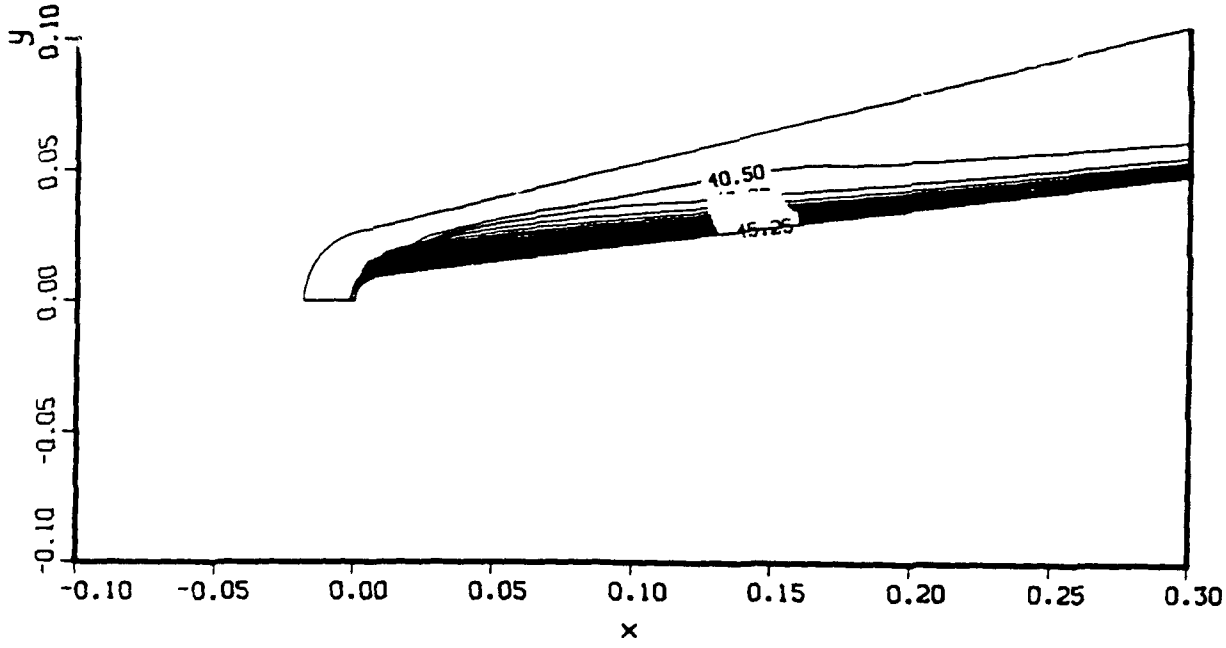

Figure 24. Enlargement of entropy contours, blunt cone at Mach 8.

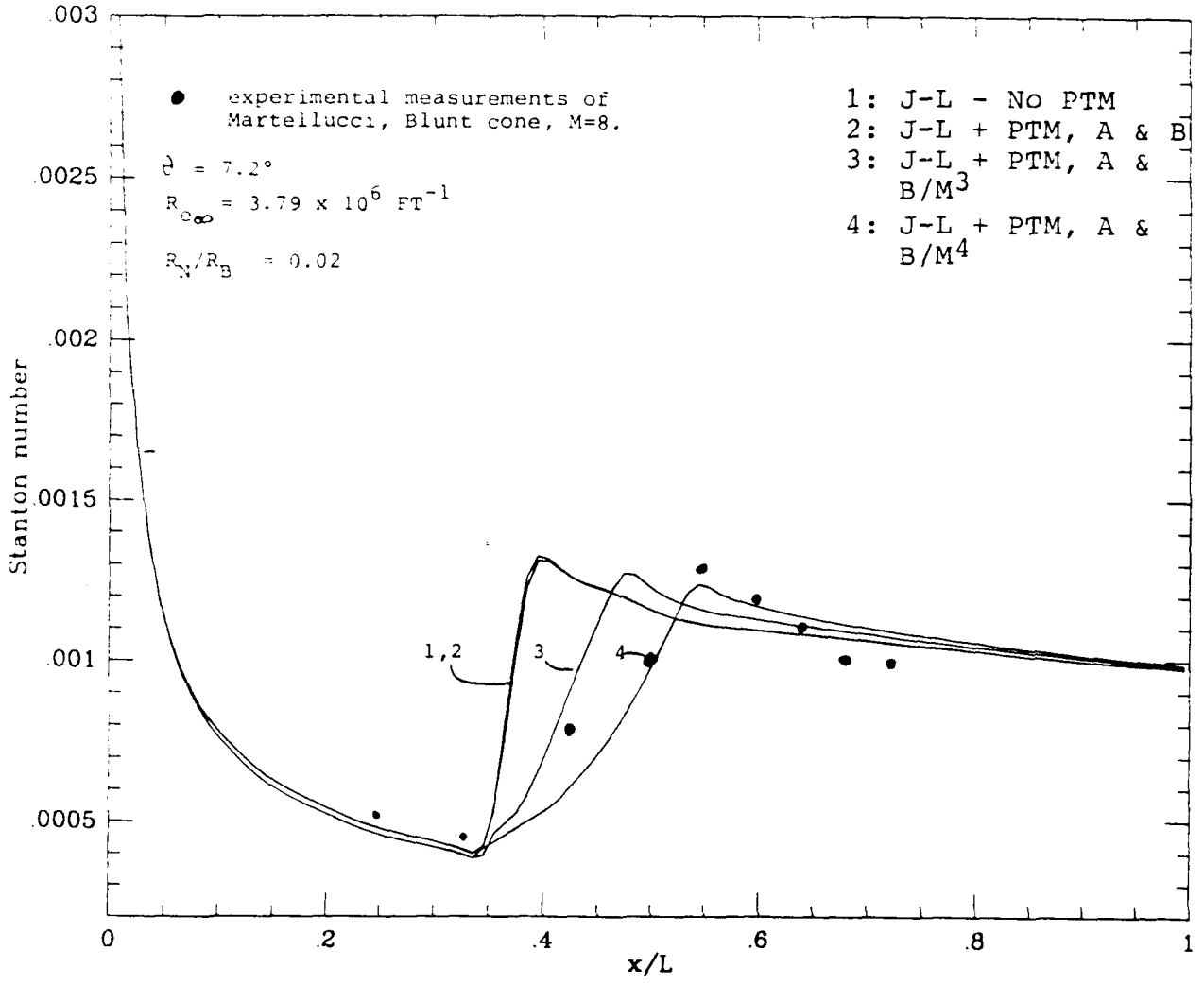

Figure 25. Calibration of A and B in the PTM model.

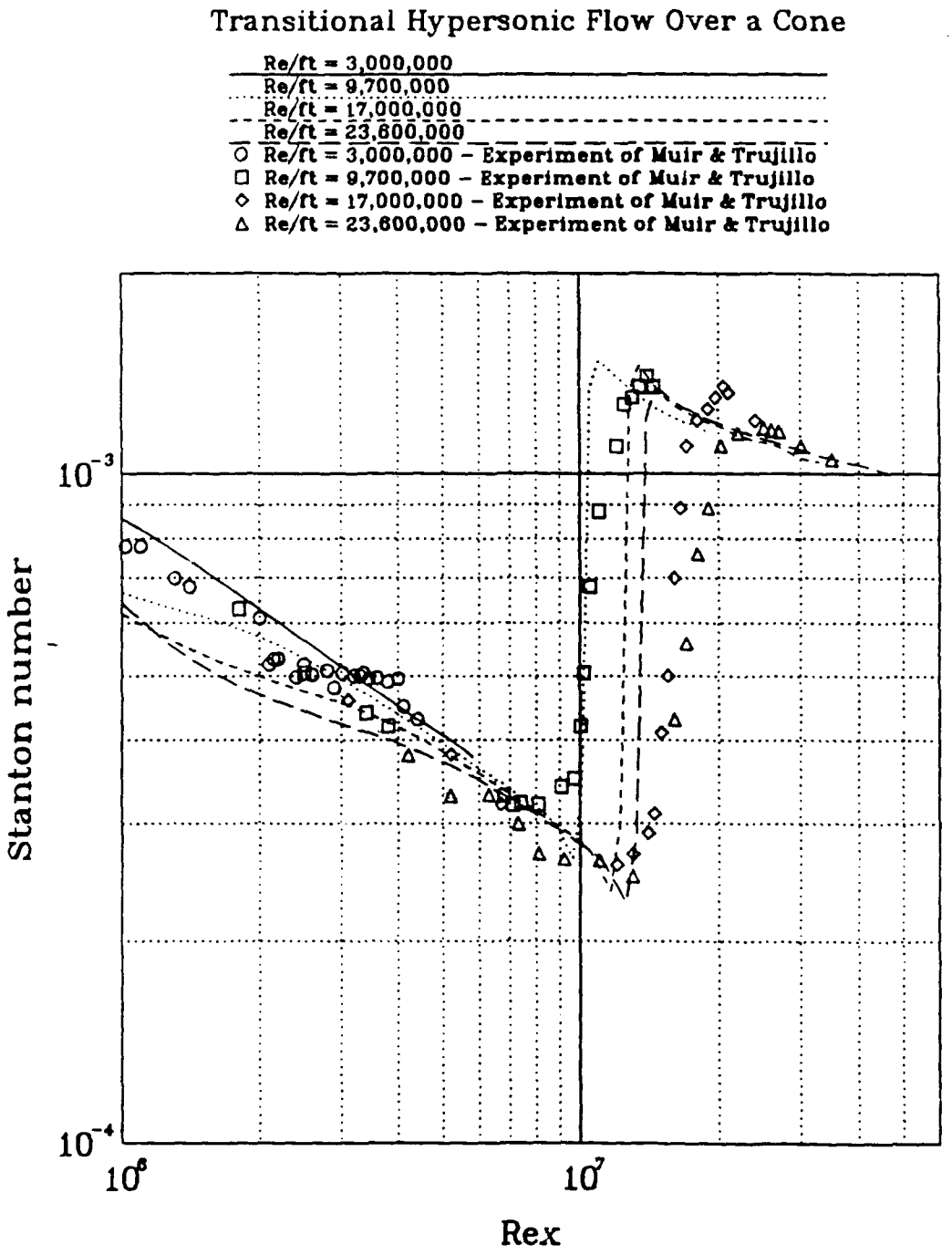

Figure 26. Variation of Stanton number with free-stream Reynolds number for a blunt cone, RN=0.1 in., no transition model used.

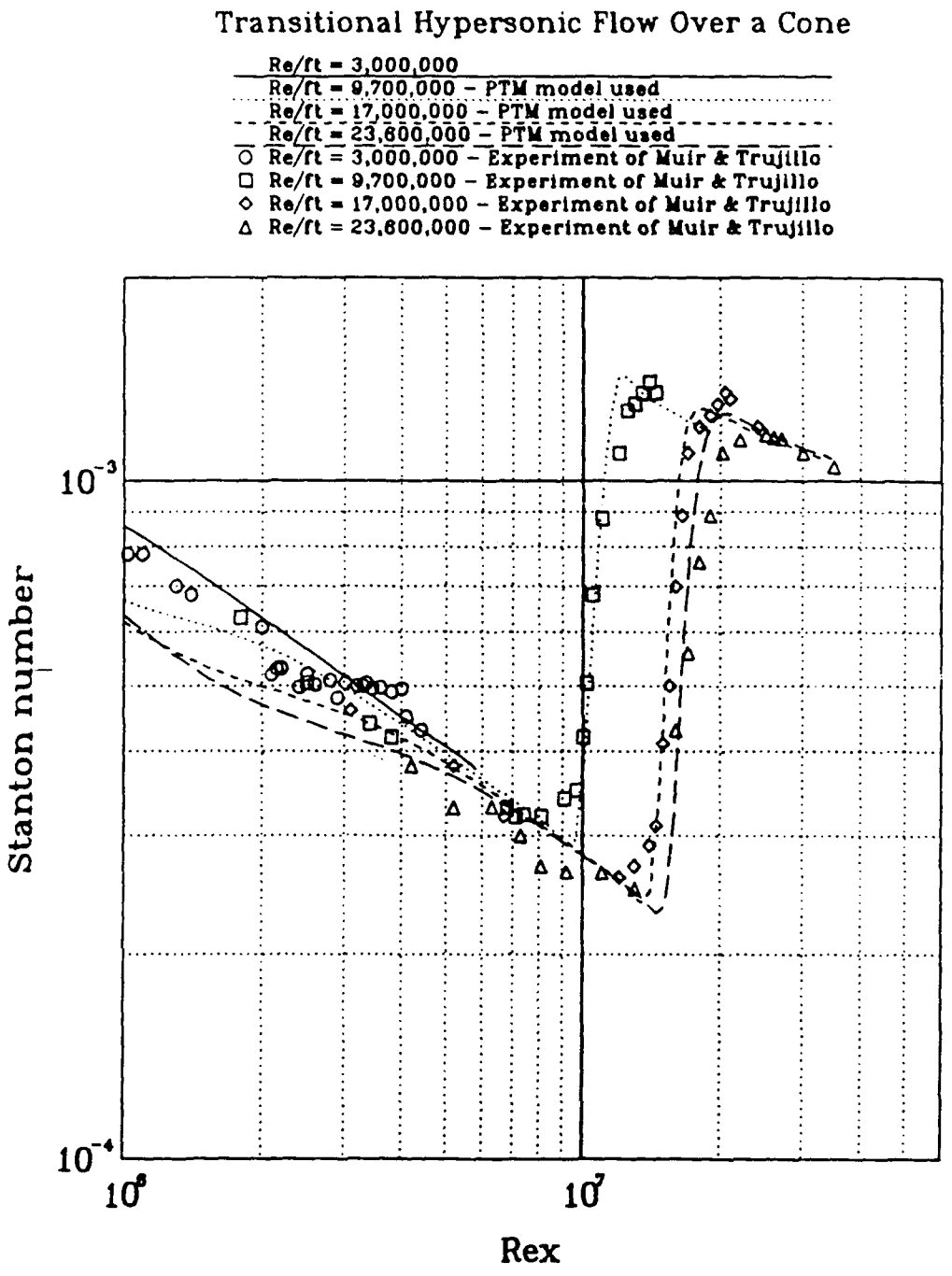

Figure 27. Variation of Stanton number with free-stream Reynolds number for a blunt cone, RN=0.1 in. - PTM model used.